

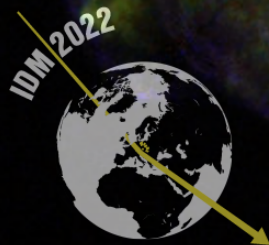
# Charged-particle

## What charged cosmic rays tell us on dark matter

Pierre Salati – LAPTh & Université Savoie Mont Blanc

### Outline

- 1) Dark matter and antimatter cosmic rays
- 2) Measuring the height  $L$  of the magnetic halo
- 3) Positrons, dark matter and TeV haloes
- 4) Antiprotons – Trimmed hints and robust bounds
- 5) Anti-He nuclei – The new frontier



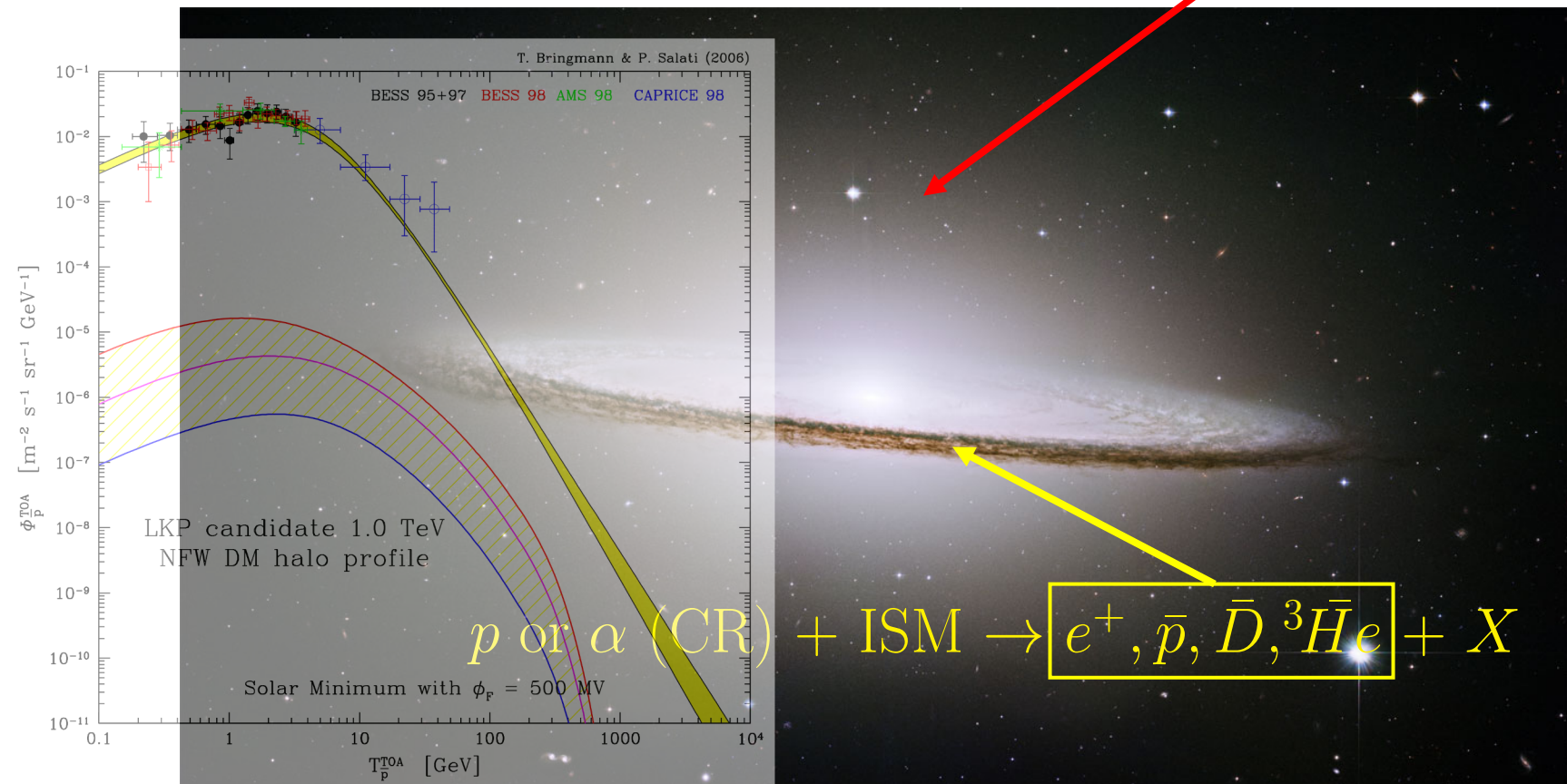
14th International Conference on  
Identification of Dark Matter

18-22 July 2022  
Vienna, Austria

# 1) Dark matter and antimatter cosmic rays

**Dark Matter particles** could be the major component of the haloes of galaxies. Their mutual annihilations or decays would produce an **indirect signature** under the form of high-energy **cosmic rays**.

$$\chi + \chi \rightarrow q\bar{q}, W^+W^-, \dots \rightarrow \gamma, e^+, \bar{p}, \bar{D}, {}^3\bar{H}e \text{ \& } \nu's$$



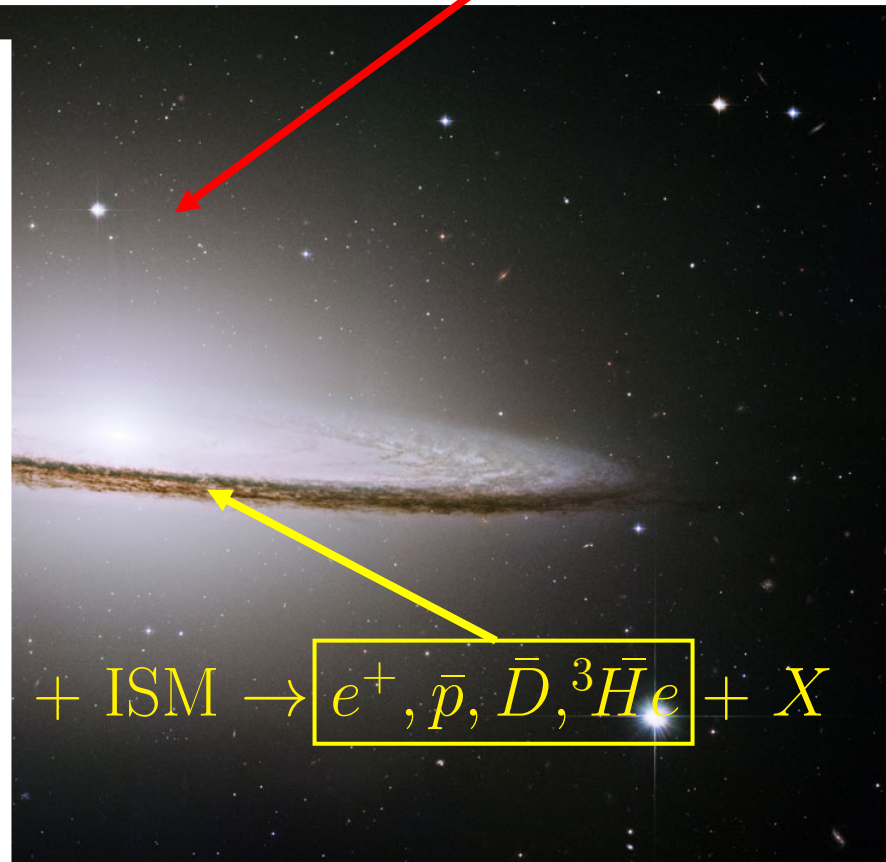
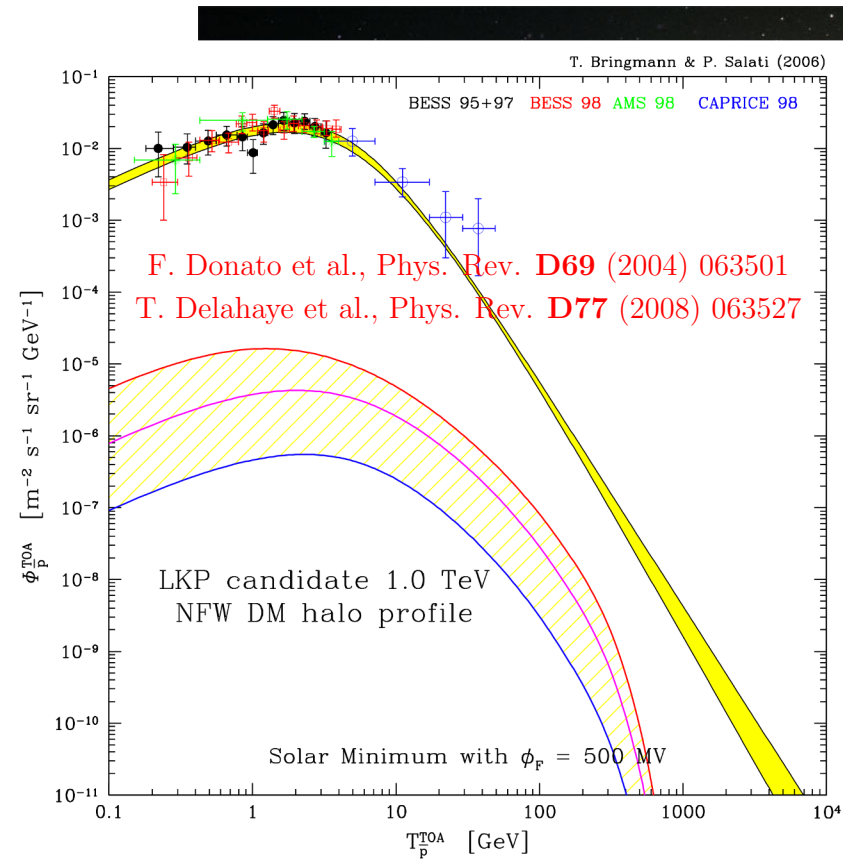
**Uncertainties** from **cosmic ray propagation** need to be ascertained. Among them, the **size  $L$  of the magnetic halo** plays a crucial role.



# 1) Dark matter and antimatter cosmic rays

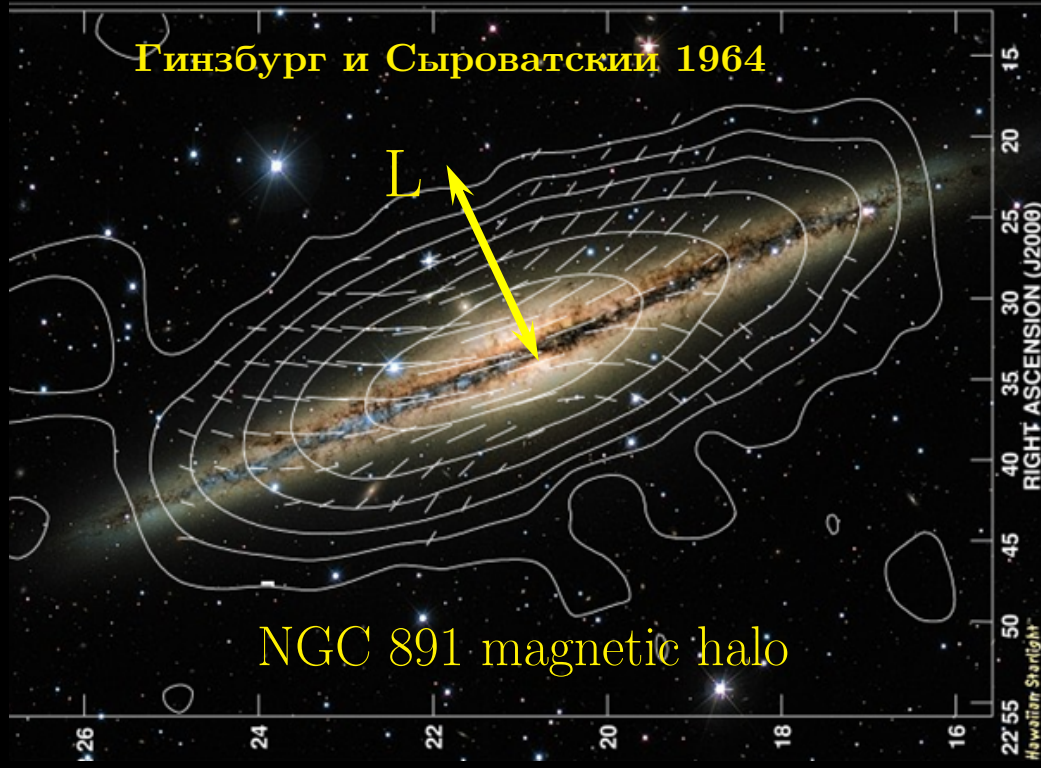
**Dark Matter particles** could be the major component of the haloes of galaxies. Their mutual annihilations or decays would produce an **indirect signature** under the form of high-energy **cosmic rays**.

$$\chi + \chi \rightarrow q\bar{q}, W^+W^-, \dots \rightarrow \gamma, e^+, \bar{p}, \bar{D}, {}^3\bar{H}e \text{ \& } \nu's$$



**Uncertainties** from **cosmic ray propagation** need to be ascertained. Among them, the **size  $L$  of the magnetic halo** plays a crucial role.

## 2) Measuring the height $L$ of the magnetic halo



$$\psi = \frac{dn}{dE} = \frac{d^4N}{d^3x dE}$$

$$\Phi = \frac{1}{4\pi} v \psi$$

$$(\text{GeV/nuc})^{-1} \text{ cm}^{-2} \text{ s}^{-1} \text{ sr}^{-1}$$

$$q = q_{\text{acc}}, q_{\text{sec}}, q_{\text{DM}}$$

$$\dot{\psi} + \underbrace{\nabla \cdot \{-K \nabla \psi + \psi \mathbf{V}_C\}}_{\text{convection}} + \underbrace{\frac{\partial}{\partial E} \left\{ b \psi - D_{EE} \frac{\partial \psi}{\partial E} \right\}}_{\text{E losses}} = q - \underbrace{\Gamma_d \psi - (\sigma v n_H) \psi}_{\text{decay \& ISM spallation}}$$

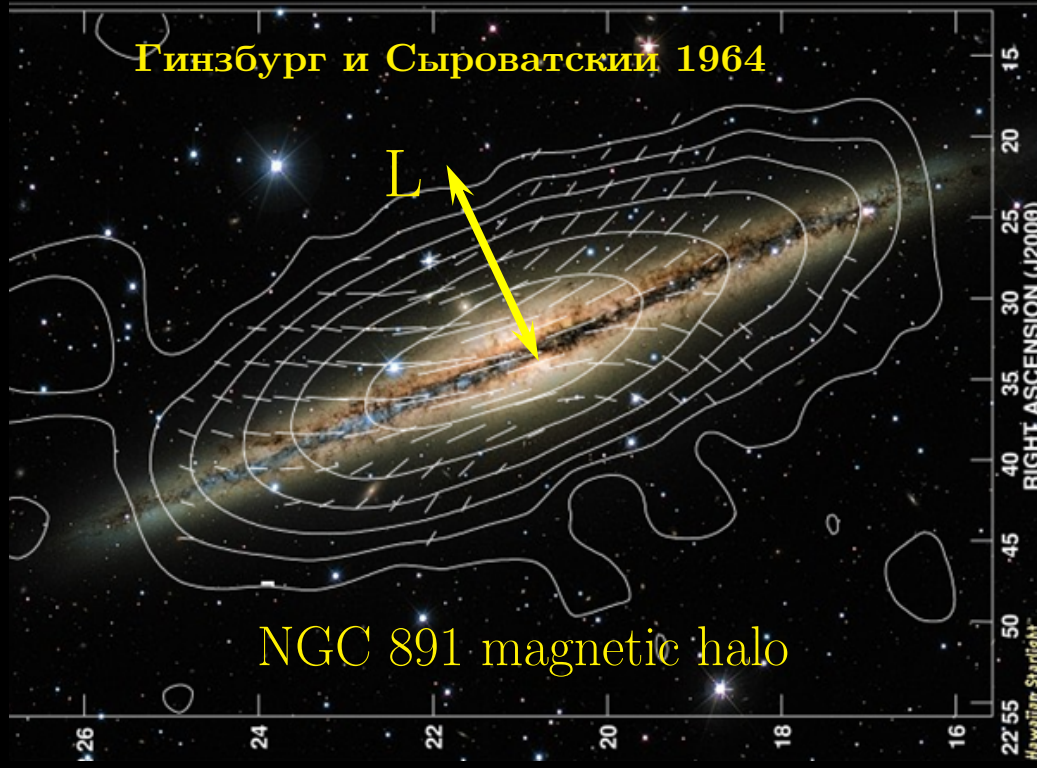
$x$  diffusion

E diffusion

$$K = \beta^\eta K_0 \left\{ 1 + \left( \frac{R_1}{R} \right)^{\frac{\delta - \delta_1}{s_1}} \right\}^{s_1} \left( \frac{R}{1 \text{ GV}} \right)^\delta \left\{ 1 + \left( \frac{R}{R_h} \right)^{\frac{\delta - \delta_h}{s_h}} \right\}^{-s_h}$$

$$D_{EE} = \frac{4}{3} \frac{\beta^2}{\delta(4 - \delta^2)(4 - \delta)} \frac{V_a^2 p^2}{K}$$

## 2) Measuring the height $L$ of the magnetic halo



$$\psi = \frac{dn}{dE} = \frac{d^4N}{d^3x dE}$$

$$\Phi = \frac{1}{4\pi} v \psi$$

$$(\text{GeV/nuc})^{-1} \text{ cm}^{-2} \text{ s}^{-1} \text{ sr}^{-1}$$

### Three CR transport schemes

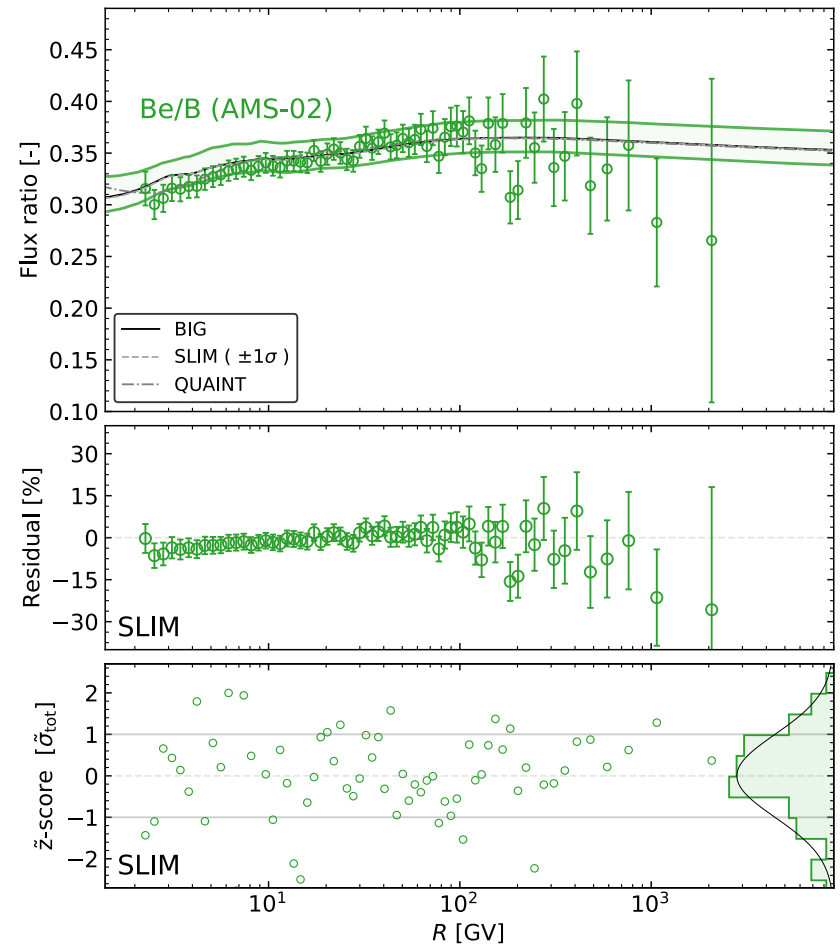
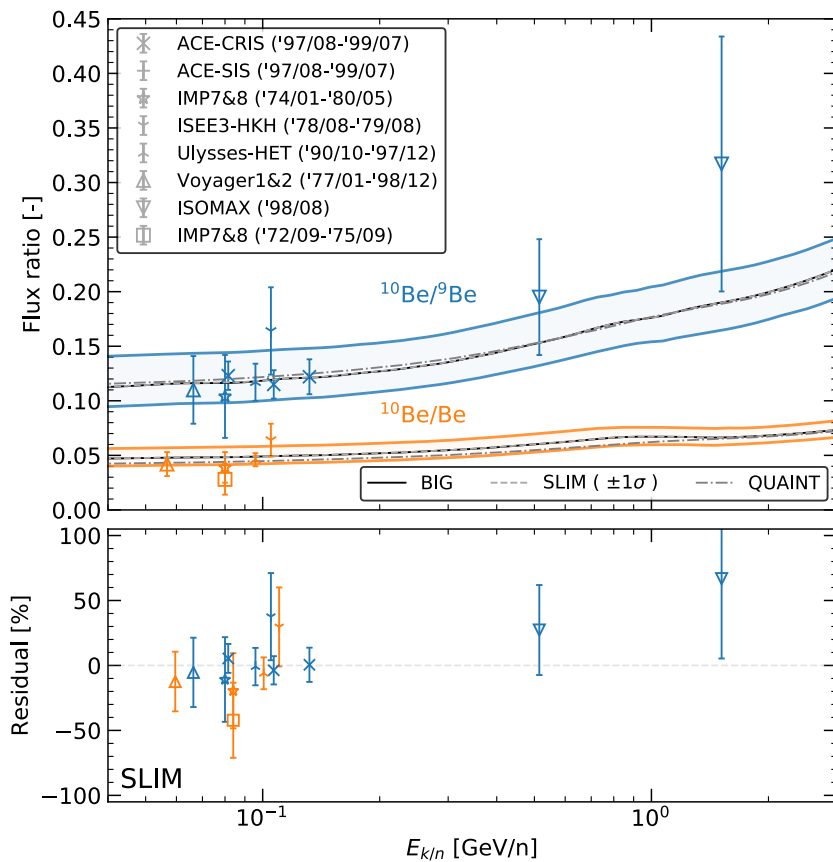
Y. Génolini et al., Phys. Rev. **D99** (2019) 123028

- **BIG** is the most comprehensive ( $K_0, \delta, R_1, \delta_1, V_C, V_a, L$ )
- **QUANT**  $\subset$  **BIG** is the old scheme ( $K_0, \delta, \eta, V_C, V_a, L$ )
- **SLIM**  $\subset$  **BIG** is for the Gifted Amateur ( $K_0, \delta, R_1, \delta_1, L$ )



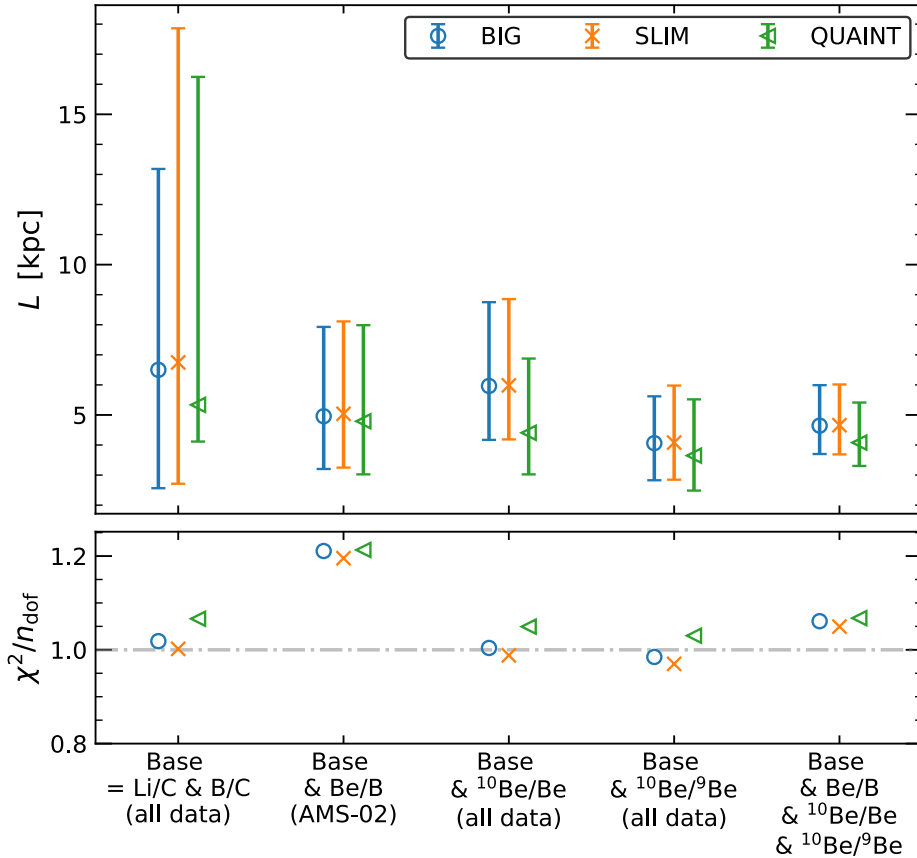
## 2) Measuring the height $L$ of the magnetic halo

- $^{10}\text{Be}$  used as a CR clock with half-lifetime  $t_{1/2}$  of 1.387 Myr
- But isotopic data at low energies and with improvable precision
- Trade-off between isotopic data  $^{10}\text{Be}/\text{Be}$  &  $^{10}\text{Be}/^9\text{Be}$  and elemental ratio  $\text{Be}/\text{B}$



Weinrich+[2002.11406] & Weinrich+2004.00441]

## 2) Measuring the height $L$ of the magnetic halo



The precision on  $L$  improves  
as more data sets are combined

	BIG	SLIM	QUAINT
<b>Base &amp; Be/B (AMS-02)</b>			
$L$ [kpc]	$4.96^{+2.97}_{-1.76}$	$5.04^{+3.07}_{-1.79}$	$4.79^{+3.19}_{-1.77}$
$\chi^2 / n_{\text{dof}}$	233.7 / 193	233.1 / 195	235.3 / 194
$\chi^2_{\text{nui}} / n_{\text{nui}}$	17.4 / 20	17.4 / 20	15.8 / 20
<b>Base &amp; Be/B &amp; <math>^{10}\text{Be}/\text{Be}</math> &amp; <math>^{10}\text{Be}/^9\text{Be}</math> (all data)</b>			
$L$ [kpc]	$4.64^{+1.35}_{-0.94}$	$4.66^{+1.35}_{-0.97}$	$4.08^{+1.33}_{-0.78}$
$\chi^2 / n_{\text{dof}}$	266.3 / 251	265.6 / 253	269.0 / 252
$\chi^2_{\text{nui}} / n_{\text{nui}}$	25.6 / 35	25.4 / 35	25.6 / 35

$\log_{10} L$     $\delta$     $\log_{10} K_0$     $V_A$     $R_1$     $\delta_1$     $V_c$   
0.667   0.498   -1.446   5.000   4.493   -1.102   0.140

( $+4.20\text{e-}3$   $+3.53\text{e-}4$   $+3.94\text{e-}3$   $+1.49\text{e-}2$   $+2.57\text{e-}3$   $-1.48\text{e-}3$   $+4.56\text{e-}2$ )  
 $+3.53\text{e-}4$   $+4.19\text{e-}4$   $+7.06\text{e-}4$   $+3.96\text{e-}3$   $+2.89\text{e-}3$   $-1.41\text{e-}3$   $+3.24\text{e-}3$   
 $+3.94\text{e-}3$   $+7.06\text{e-}4$   $+5.48\text{e-}3$   $+1.86\text{e-}2$   $+4.67\text{e-}3$   $-2.18\text{e-}3$   $+4.57\text{e-}2$   
 $+1.49\text{e-}2$   $+3.96\text{e-}3$   $+1.86\text{e-}2$   $+2.02\text{e+}1$   $+6.00\text{e-}2$   $-4.52\text{e-}2$   $+1.96\text{e-}1$   
 $+2.57\text{e-}3$   $+2.89\text{e-}3$   $+4.67\text{e-}3$   $+6.00\text{e-}2$   $+2.92\text{e-}2$   $-1.30\text{e-}2$   $+2.15\text{e-}2$   
 $-1.48\text{e-}3$   $-1.41\text{e-}3$   $-2.18\text{e-}3$   $-4.52\text{e-}2$   $-1.30\text{e-}2$   $+2.11\text{e-}2$   $-1.28\text{e-}2$   
 $+4.56\text{e-}2$   $+3.24\text{e-}3$   $+4.57\text{e-}2$   $+1.96\text{e-}1$   $+2.15\text{e-}2$   $-1.28\text{e-}2$   $+1.86\text{e+}0$ )

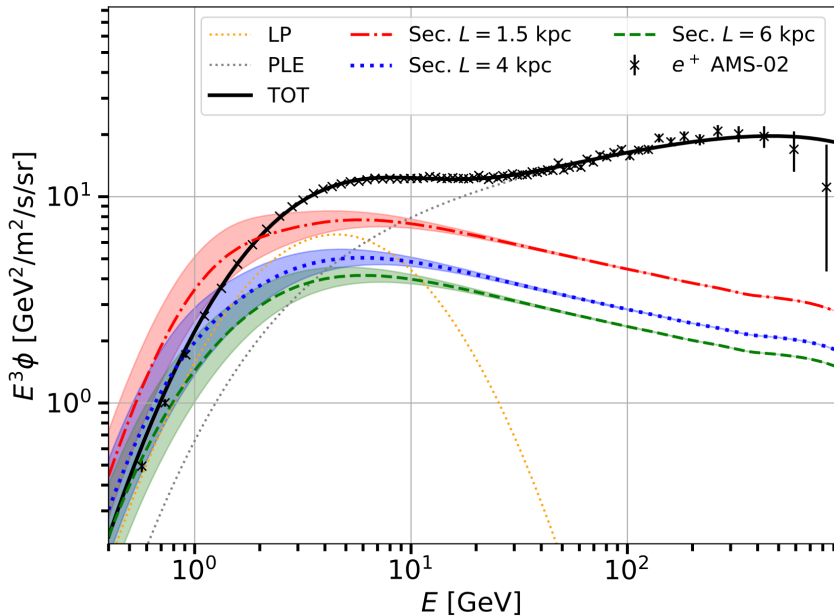
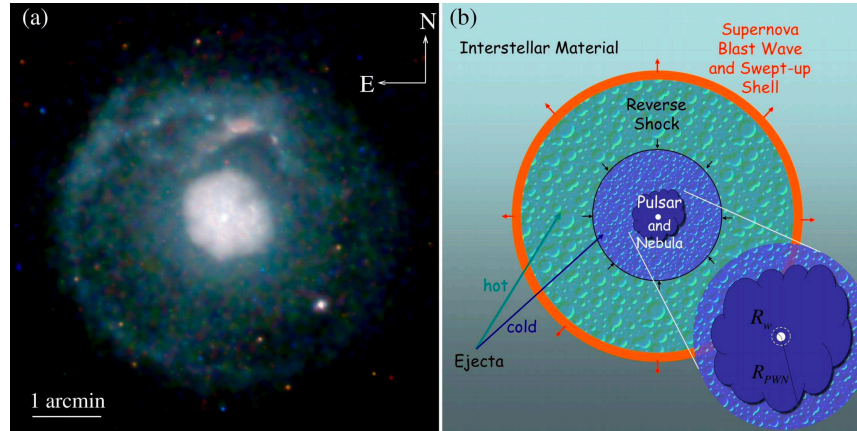
Cosmic ray parameter values and  
associated covariance matrix for BIG

Unstable secondary  $^{10}\text{Be}$  allows to measure a magnetic halo size  $L$  of  $4.5 \pm 1$  kpc

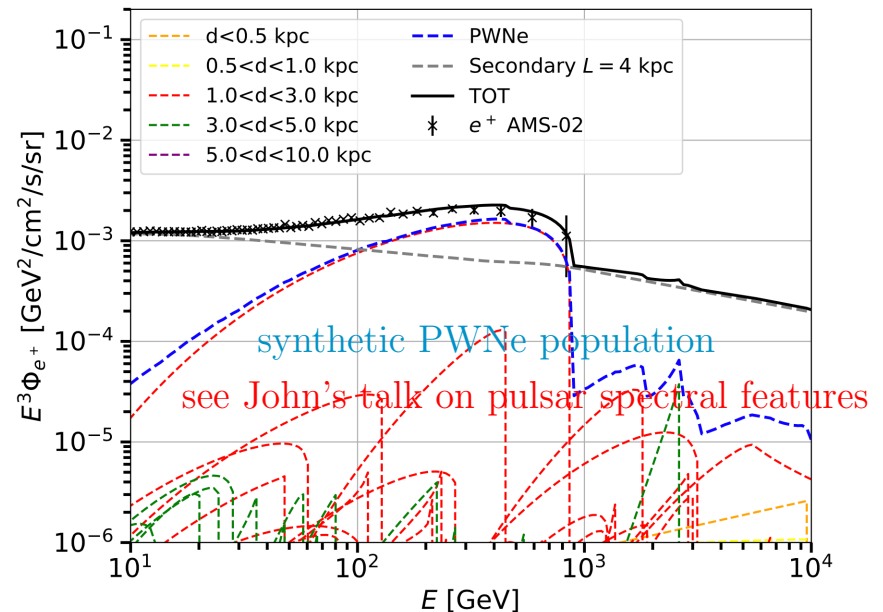
### 3) Positrons, dark matter and TeV haloes

- In 2008, the rise of the  $e^+$  fraction reported by PAMELA triggered a hectic activity to explain the excess in terms of DM. The dust has settled by now.

$$\Phi_{e^+} = \Phi_{e^+}^{\text{sec}} + \Phi_{e^+}^{\text{prim}}(\text{pulsars})$$



Di Mauro+[2101.11027]

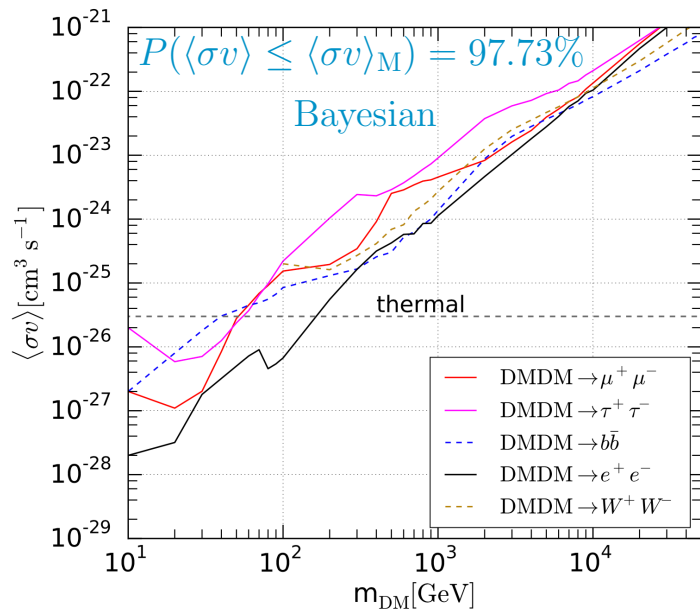
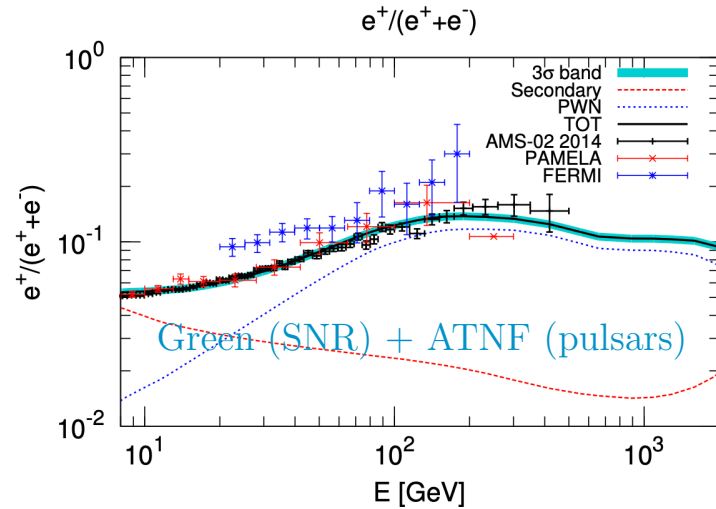
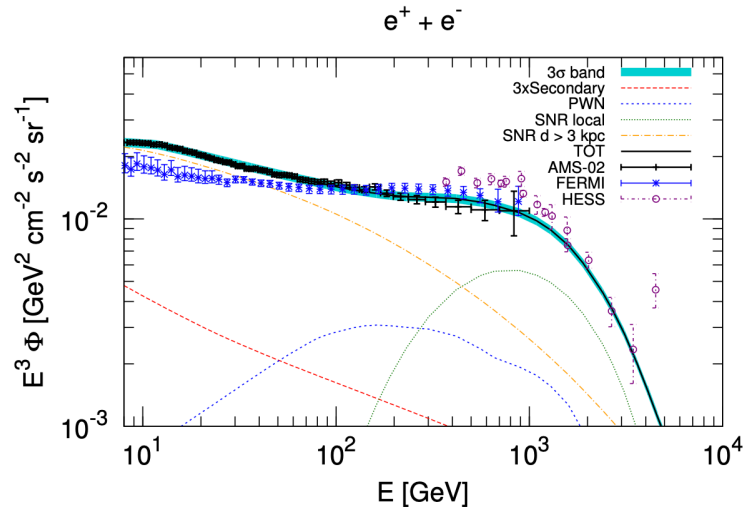


Orusa+[2107.06300]



### 3) Positrons, dark matter and TeV haloes

- In this context, setting limits on DM is challenging insofar as the pulsar contribution is not determined. We do not know the entire MW pulsar population.



Di Mauro+[1507.07001]

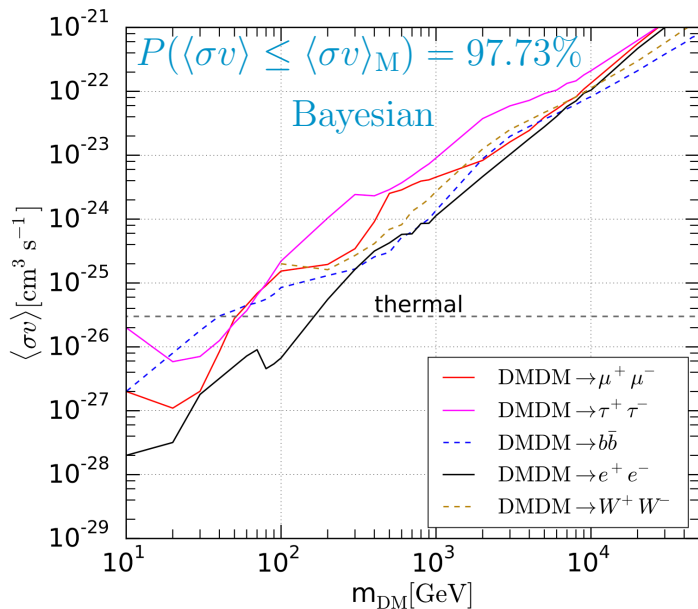
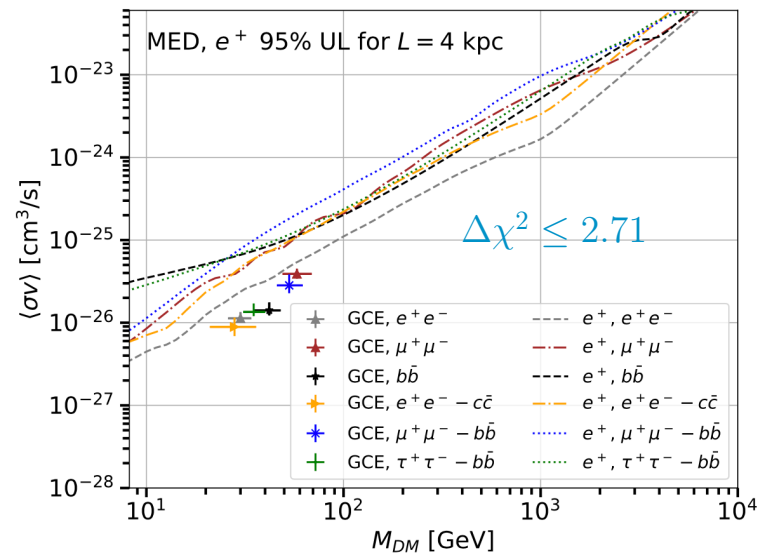
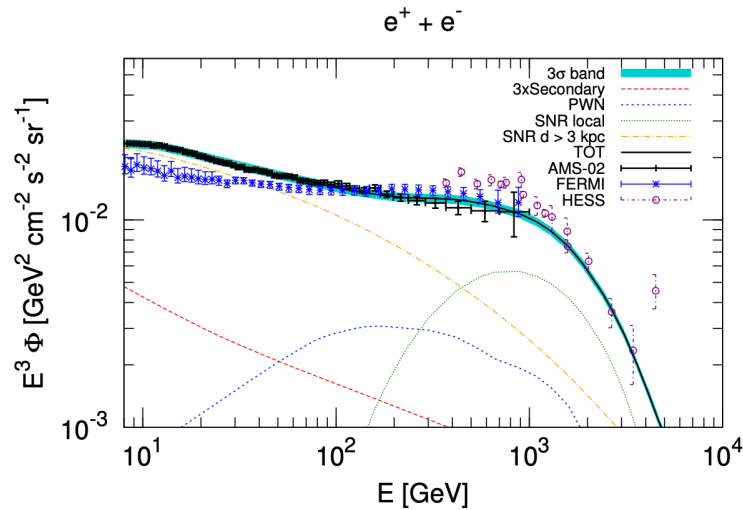
$$Q(E) = Q_{0,\text{SNRs}} \left( \frac{E}{E_0} \right)^{-\gamma_{\text{SNRs}}} \exp \left( -\frac{E}{E_c} \right)$$

$$\int_{E_{\text{min}}}^{\infty} dE E Q(E) = \eta_{\text{PWNe}} W_0$$

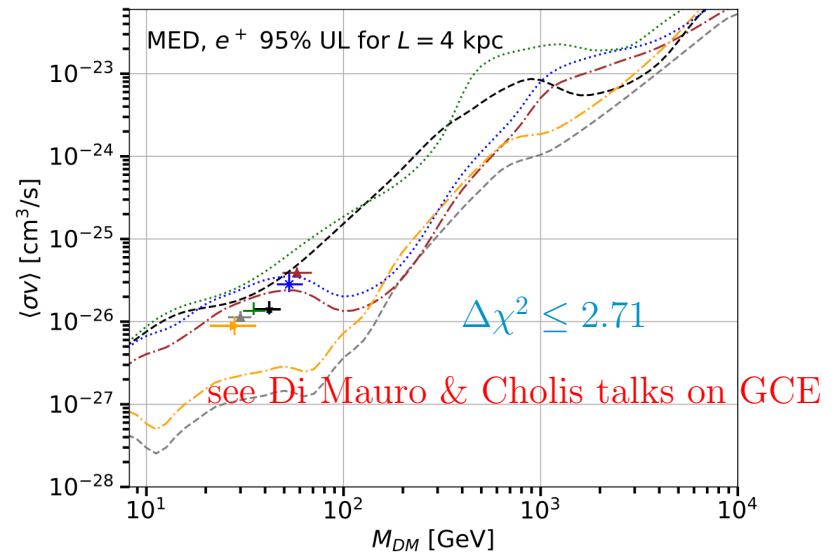
parameter	all 4 datasets	only PF and SUM	only $e^+$ and $e^-$ fluxes
$\eta_{\text{PWNe}}$	$0.037^{+0.001}_{-0.001}$	$0.036^{+0.002}_{-0.001}$	$0.037^{+0.001}_{-0.002}$
$\gamma_{\text{PWNe}}$	$1.95^{+0.03}_{-0.02}$	$1.94^{+0.04}_{-0.02}$	$1.95^{+0.2}_{-0.2}$
$Q_{0,\text{SNRs}}$ [10 <sup>50</sup> erg/s]	$1.23^{+0.01}_{-0.03}$	$1.10^{+0.15}_{-0.05}$	$1.26^{+0.06}_{-0.09}$
$\gamma_{\text{SNRs}}$	$2.24^{+0.02}_{-0.01}$	$2.22^{+0.02}_{-0.01}$	$2.24^{+0.01}_{-0.01}$
$N_{\text{Vela}}$	$0.98^{+0.03}_{-0.13}$	$1.00^{+0.23}_{-0.19}$	$0.93^{+0.14}_{-0.16}$
$\chi^2_{\text{tot}}/\text{d.o.f}$	1.03	1.35	0.76
$\chi^2_{\text{pf}}$ (43 data pts)	81.7	80.4	-
$\chi^2_{\text{sum}}$ (50 data pts)	36.0	37.2	-
$\chi^2_{e^+}$ (49 data pts)	39.7	-	40.4
$\chi^2_{e^-}$ (49 data pts)	33.6	-	28.9

### 3) Positrons, dark matter and TeV haloes

- In this context, setting limits on DM is challenging insofar as the pulsar contribution is not determined. We do not know the entire MW pulsar population.



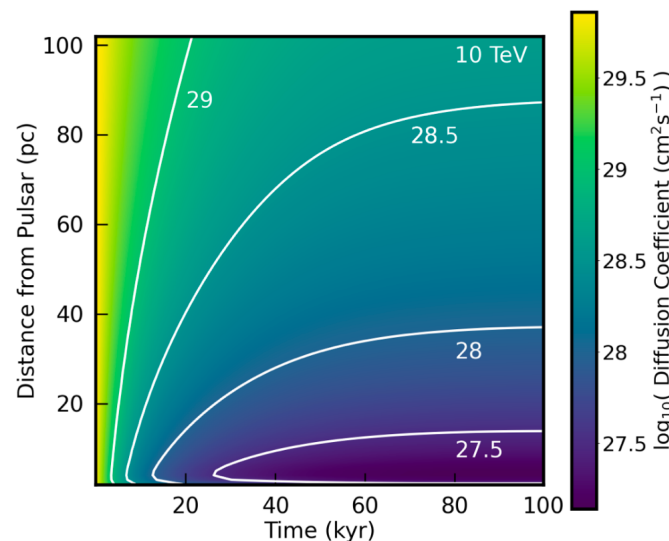
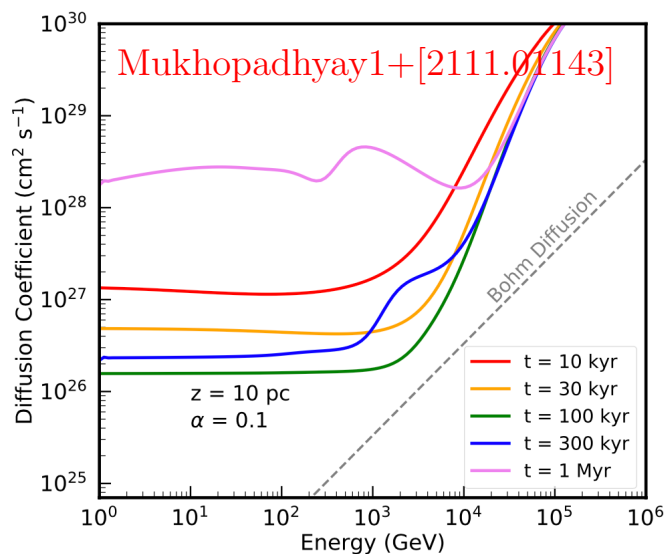
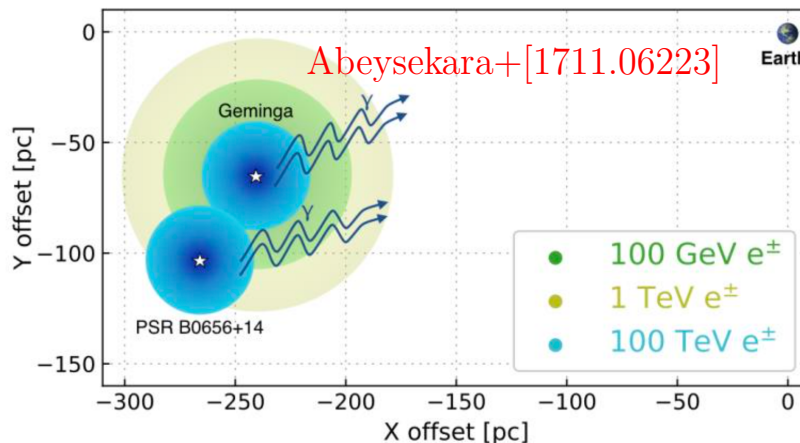
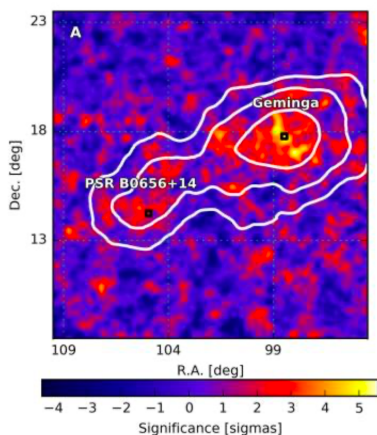
Di Mauro+[1507.07001]



Di Mauro+[2101.11027]

### 3) Positrons, dark matter and TeV haloes

- TeV haloes have been discovered around pulsars, with  $\gamma$ -rays from the ICS of  $e^\pm$ . This indicates that pulsars accelerate these species. CR diffusion is much slower inside these regions.



CR generate themselves the magnetic turbulence inside which they are trapped.



## 4) Antiprotons – Trimmed hints and robust bounds

Over the past few years, many analyses concluded that  $\Phi_{\bar{p}}$  hints at DM

Authors	Data analyzed	Method F or B	$\mathcal{C}^{\text{data}}$	$\mathcal{C}^{\text{model}}$	Significance of fit w and w/o DM	Conclusive hint for DM
Cuoco+[1610.03071]	$\bar{p}/p, p$ & He + Voyager $p$ & He	F	no	no	$4.7 \sigma$ (L,2dof)	yes
Cui+[1610.03840]	$\bar{p}$ with prior $\Pi(\lambda)$ from CR nuclei	B	no	no	$2 \ln K = 11$ to 54	Decisive
Reinert+[1712.00002]	B/C, $\bar{p}$ & AMS/PAM	F	no	$\mathcal{C}^{\text{XS,parents}}$	$2.2 \sigma$ (L,1dof) $\rightarrow$ $1.1 \sigma$ (G)	no
Cui+[1805.11590]	$\bar{p}$ with prior $\Pi(\lambda)$ from CR nuclei + PandaX-II, LUX, XENON1T (DD)	B	no	no	Best-fit $m_\chi$ and $\langle \sigma v \rangle$	N/A
Cuoco+[1903.01472]	$\bar{p}/p, p$ & He + Voyager and CREAM $p$ & He all data with $\mathcal{R} > 5$ GV	F	no	no	$3.1 \sigma$ (L,2dof)	yes
		F	no	$\mathcal{C}^{\text{XS}}$	$2.9 \sigma$ (L,2dof)	yes
		F	✓	no	$5.5 \sigma$ (L,2dof)	yes
Cholis+[1903.02549]	$\bar{p}/p$ with best-fit of fudge factor $N_{XS}(T_{\bar{p}})$ + $\bar{p}$ production in SNR shocks	F	no	no	$4.7 \sigma$ (L,1dof)	yes
		F	no	no	$3.3 \sigma$ (L,1dof)	yes
Heisig+[2005.04237]	B/C, $\bar{p}$ & AMS/PAM $\bar{p}/p, p$ & He + Voyager $p$ & He	F	✓	$\mathcal{C}^{\text{XS}}$	$0.5 \sigma$ (L,1dof)	no
		F	✓	$\mathcal{C}^{\text{XS}}$	$1.8 \sigma$ (L,1dof) $\rightarrow$ $0.5 \sigma$ (G)	no
Di Mauro+[2101.11027]	B/C, $\bar{p}$ & AMS/PAM	F	✓	$\mathcal{C}^{\text{XS}}$	$2 \sigma$ (L,1dof) $\rightarrow$ $1 \sigma$ (G)	no
Luque+[2107.06863]	B/C, B/O, Be/C, Be/O, Be/B, Li/B, Li/Be + $^{10}\text{Be}/\text{Be}$ , $^{10}\text{Be}/^9\text{B}$ and $\bar{p}/p$	B	no	no	DM fit is poorer than fit w/o DM	no
Kahlhoefer+[2107.12395]	$p, \text{He}$ & $\bar{p}/p$ + Voyager $p$ & He	F+B	no	no	$4.5 \sigma$ (L,1dof)	TBC
Calore+[2202.03076]	$\bar{p}$ + nuisance on $L$ from LiBeB	F	✓	✓	$1.8 \sigma$ (L,1dof)	no

The differences in conclusion do not lie in the CR transport codes (Galprop, DRAGON or USINE) nor in the statistical approach (frequentist or Bayesian). They originate from the treatment of errors Calore+[2202.03076].

## $\bar{p}$ – Methodology and the definition of the likelihood

- We use the likelihood ratio  $LR$  which provides a powerful estimator for testing the null-hypothesis and deriving DM constraints.

$$LR(\text{null}) = -2 \ln \left\{ \frac{\sup_{\lambda \in \Lambda} \mathcal{L}(\lambda)}{\sup_{\{\lambda, \mu\} \in \Lambda \cup M} \mathcal{L}(\lambda, \mu)} \right\} \quad \text{while} \quad LR(\mu_0) = -2 \ln \left\{ \frac{\sup_{\lambda \in \Lambda} \mathcal{L}(\lambda, \mu_0)}{\sup_{\{\lambda, \mu\} \in \Lambda \cup M} \mathcal{L}(\lambda, \mu)} \right\}$$

Here  $\lambda \in \Lambda$  stands for the CR parameters while  $\mu \equiv \{m_\chi, \langle \sigma v \rangle, \text{channel}\}$ .

- Defining the likelihood function  $\mathcal{L}(\lambda, \mu)$  requires some care. In principle, we could define it through a *global*  $\chi^2$  measuring the distance of both nuclear and antiproton data to theory.

$$-2 \ln \mathcal{L}(\lambda, \mu) \equiv \chi_{\text{LiBeB}}^2(\lambda) + \chi_{\bar{p}}^2(\lambda, \mu)$$

- This would be extremely CPU-time and resources consuming. A close inspection to the  $\bar{p}$  flux is mandatory to define a more tractable yet robust likelihood.

$$\Phi_{\bar{p}} = \Phi_{\bar{p}}^{\text{sec}}(\lambda) + \Phi_{\bar{p}}^{\text{DM}}(\lambda, \mu)$$

$\Phi_{\bar{p}}^{\text{sec}}$  dominates over  $\Phi_{\bar{p}}^{\text{DM}}$  and behaves like a stable secondary nuclear species. CR parameters  $\hat{L}$  and  $\hat{\lambda}_i$  minimizing  $\chi_{\text{LiBeB}}^2$  should also minimize  $\chi_{\bar{p}}^2$ . Actually for BIG, NFW and  $b\bar{b}$ , we get

$$\hat{L} = 4.96 \text{ kpc vs } L_{\text{sec}} = 5.00 \text{ kpc vs } L^* = 4.38 \text{ kpc}$$

See also [Boudaud+\[1906.07119\]](#).

# $\bar{p}$ – Methodology and the definition of the likelihood

- We replace  $\chi_{\text{LiBeB}}^2(\lambda)$  by the posterior probability  $\Pi(\lambda)$  yielded by the LiBeB analysis on CR parameters  $\lambda \equiv \{L, \lambda_i\}$ . We consider this posterior PDF as a prior for the  $\bar{p}$  analysis. Several possibilities to incorporate it.

$$\mathcal{P}(\mu) \propto \int \mathcal{L}(\bar{p} | \mu, \lambda) \Pi(\lambda) d\lambda \quad \text{Bayesian, see Cui+[1805.11590]}$$

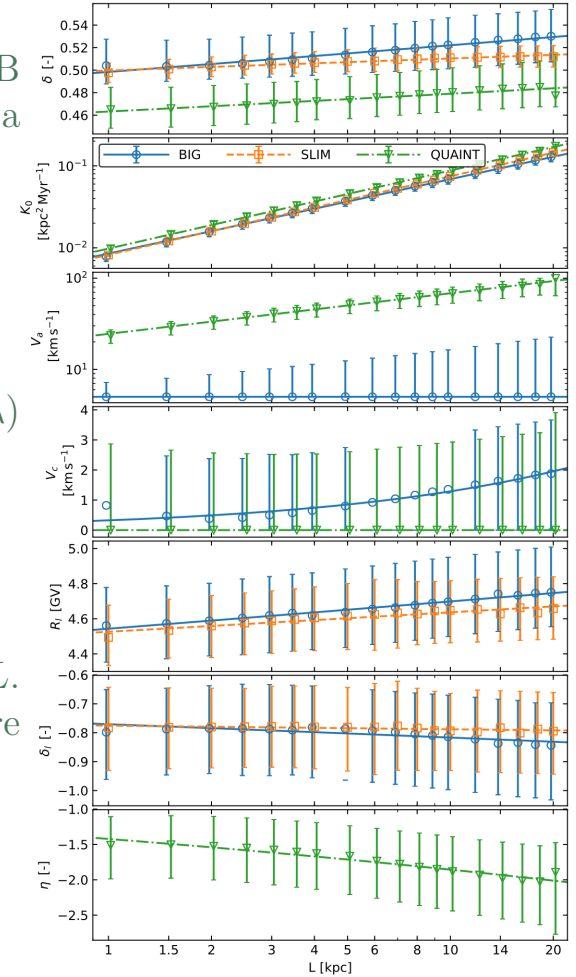
- Another option is to generate the multivariate normal distribution of  $\Phi_{\bar{p}}(\lambda)$  with covariance matrix  $\mathcal{C}^{\text{model}}$  calculated from

$$\mathcal{C}_{ij}^{\text{model}} = \langle \Phi_{\bar{p},i}^{\text{th}} \Phi_{\bar{p},j}^{\text{th}} \rangle - \langle \Phi_{\bar{p},i}^{\text{th}} \rangle \langle \Phi_{\bar{p},j}^{\text{th}} \rangle \quad \text{see Boudaud+[1906.07119]}$$

- We also remark that  $\Phi_{\bar{p}}^{\text{DM}} \propto L^2/K \propto L$  is very sensitive to halo size  $L$ . We split CR parameters. Halo size goes in the definition of  $\mathcal{L}$  while  $\lambda_i$  are incorporated in  $\mathcal{C}^{\text{model}}$ . This leads to the definition

$$-2 \ln \mathcal{L}(\lambda, \mu) \equiv -2 \ln \mathcal{L}(L, \mu) = \left\{ \frac{\log L - \log \hat{L}}{\sigma_{\log L}} \right\}^2 + \{ \chi_{\bar{p}}^2 \equiv x_i (\mathcal{C}^{-1})_{ij} x_j \}$$

- The CR parameters  $\lambda_i$  are set at their LiBeB maximum likelihood values for each halo size  $L$ .



$$\text{parameter } \lambda_i(L) = A_i \left\{ \frac{L}{5 \text{ kpc}} \right\}^{B_i}$$

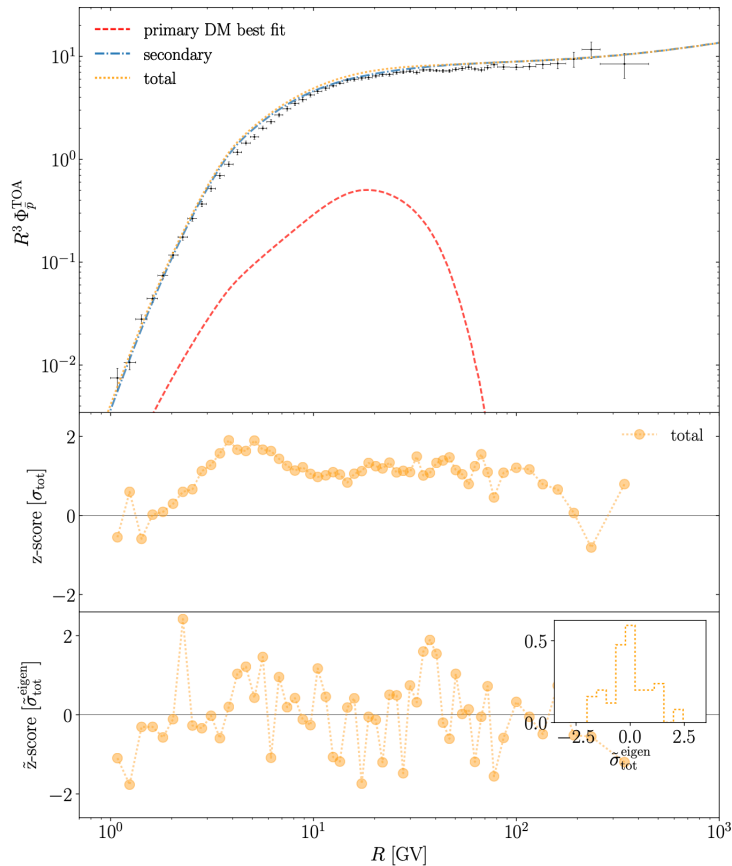
Weinrich+2004.00441]



# $\bar{p}$ – Exploring the null hypothesis in search for DM

Taking into account the previous construction, we define the likelihood ratio as

$$LR(\text{null}) = -2 \ln \mathcal{L}(L_{\text{sec}}, \langle \sigma v \rangle \equiv 0) + 2 \ln \mathcal{L}(L^*, m^*, \langle \sigma v \rangle^*)$$



DM best fit for  $b\bar{b}$  channel, NFW and BIG

Final state	Model	$m^*$ [GeV]	$\langle \sigma v \rangle^*$ [cm <sup>3</sup> /s]	$LR$ (denom)	$LR$ (num)	$LR$	local signif. [ $\sigma$ ]
$b\bar{b}$	BIG	109.3	1.71e-26	48.37	51.65	3.28	1.8
$b\bar{b}$	SLIM	109.1	1.48e-26	48.77	51.70	2.93	1.7
$b\bar{b}$	QUAINT	106.7	4.28e-27	45.32	45.53	0.22	0.5
$q\bar{q}$	BIG	88.5	4.41e-27	50.31	51.65	1.35	1.2
$\mu^+\mu^-$	BIG	155.7	2.65e-23	49.76	51.65	1.90	1.4
$W^+W^-$	BIG	106.8	2.20e-26	49.24	51.65	2.41	1.6
$hh$	BIG	166.7	3.62e-26	49.28	51.65	2.38	1.5

dof = 54      56

**Beware of a naive interpretation**

We are tempted to gauge the statistical significance of the null hypothesis by interpreting  $LR$  as a  $\Delta\chi^2$  with 2 degrees of freedom, i.e.  $m_\chi$  and  $\langle \sigma v \rangle$ , but this is wrong.



In data space,  $m_\chi$  and  $\langle \sigma v \rangle$  do not span a 2D plane since we get the same theoretical point for  $\langle \sigma v \rangle \equiv 0$  for all  $m_\chi$ .

The DM mass  $m_\chi$  is **not** defined under the null hypothesis.

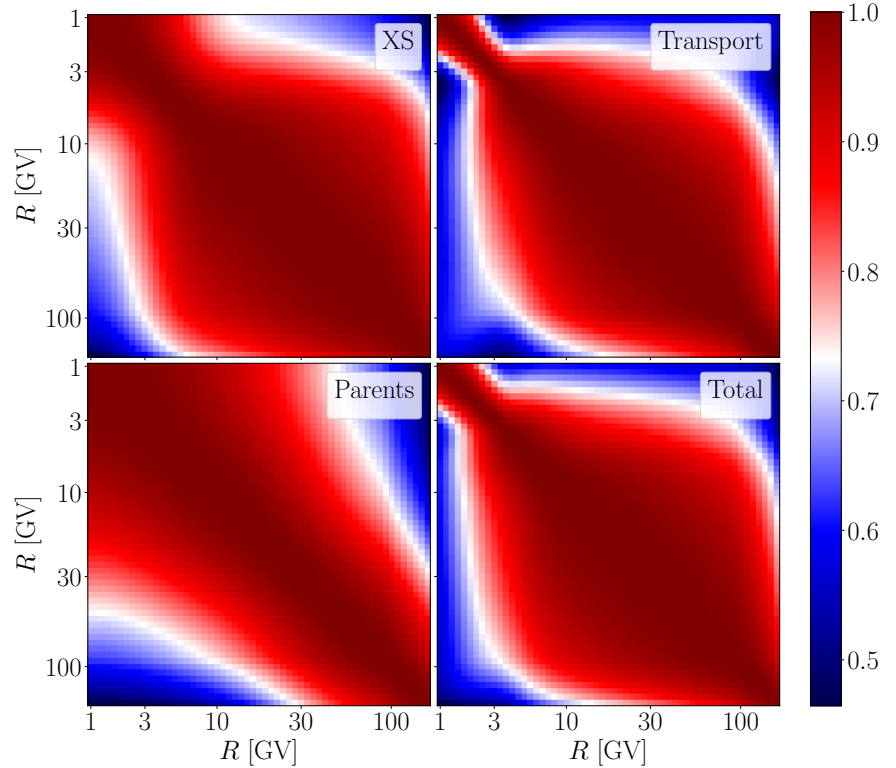
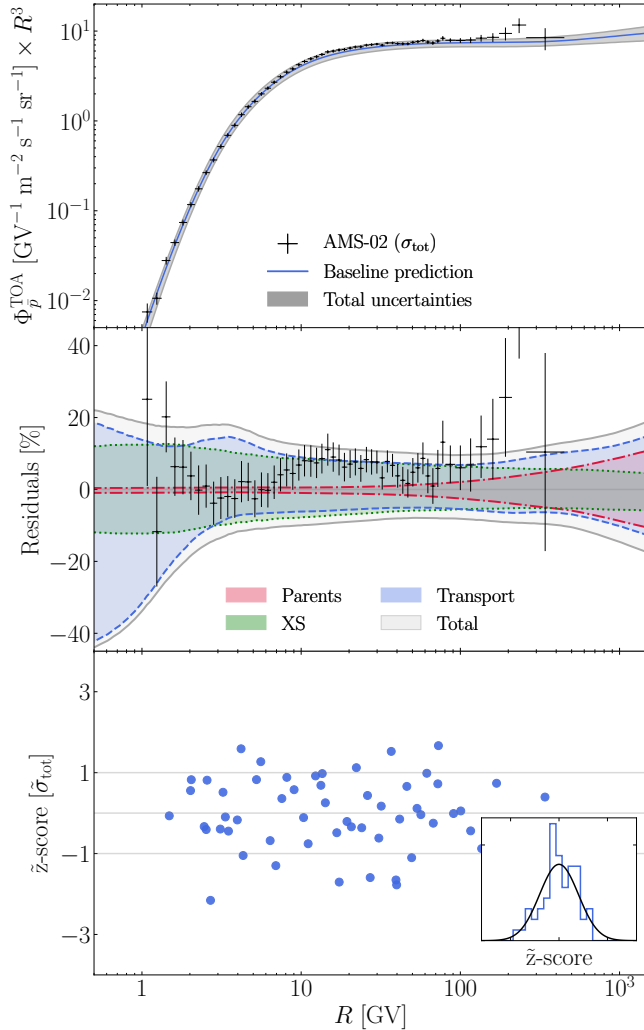
The **global** significance is determined by generating mock  $\bar{p}$  data under the null hypothesis (only secondaries) to build the  $\Delta\chi^2$  distribution and gauge the actual  $p$ -value. Heisig+[2005.04237] find 1.8  $\sigma$  (local) yielding 0.5  $\sigma$  (global).

# $\bar{p}$ – Exploring the null hypothesis in search for DM

Results vary among authors. Errors on  $\bar{p}$  flux should be dealt with great care.

$$\chi_{\bar{p}}^2 \equiv x_i (\mathcal{C}^{-1})_{ij} x_j \quad \text{where } x_i = \Phi_{\bar{p},i}^{\text{exp}} - \Phi_{\bar{p},i}^{\text{th}} \quad \text{while } \mathcal{C} = \mathcal{C}^{\text{data}} + \mathcal{C}^{\text{model}}$$

Boudaud+[1906.07119]



$$\text{Covariance matrix } \mathcal{C}^{\text{model}} = \sum_{\alpha} \mathcal{C}^{\alpha} = \mathcal{C}^{\text{XS}} + \mathcal{C}^{\text{transport}} + \mathcal{C}^{\text{parents}}$$

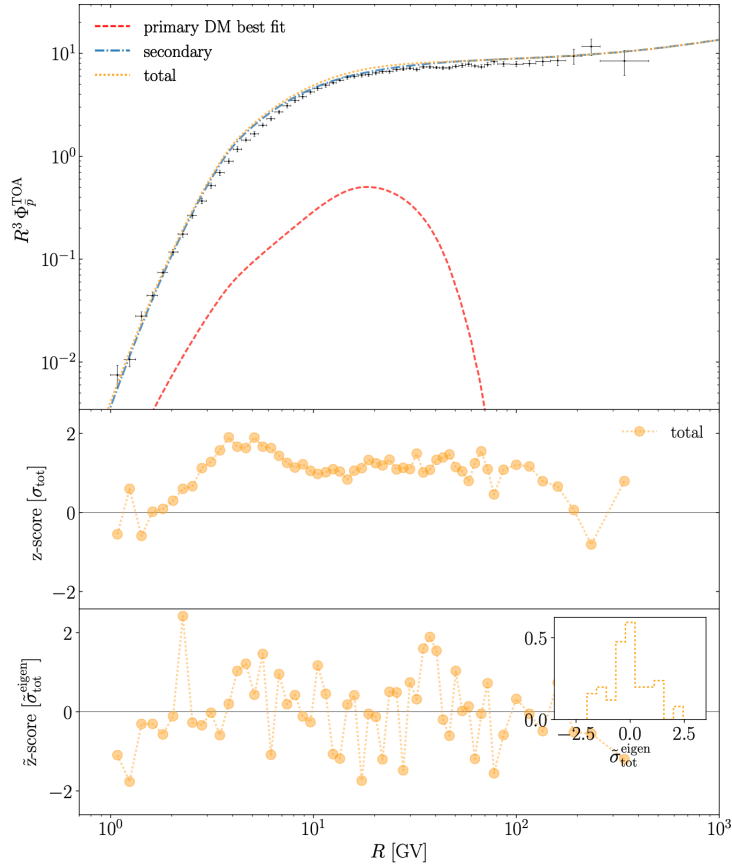
$$\text{Each component is obtained from } \mathcal{C}_{ij}^{\alpha} = \frac{1}{N} \sum_{n=1}^N (\Phi_{i,n}^{\alpha} - \mu_i^{\alpha}) (\Phi_{j,n}^{\alpha} - \mu_j^{\alpha})$$

$$\text{The correlation matrix is defined as } c_{ij}^{\alpha} = \frac{\mathcal{C}_{ij}^{\alpha}}{\sqrt{\mathcal{C}_{ii}^{\alpha}} \sqrt{\mathcal{C}_{jj}^{\alpha}}} \quad \text{with } |c_{ij}^{\alpha}| \leq 1$$

# $\bar{p}$ – Exploring the null hypothesis in search for DM

Taking into account the previous construction, we define the likelihood ratio as

$$LR(\text{null}) = -2 \ln \mathcal{L}(L_{\text{sec}}, \langle \sigma v \rangle \equiv 0) + 2 \ln \mathcal{L}(L^*, m^*, \langle \sigma v \rangle^*)$$



DM best fit for  $b\bar{b}$  channel, NFW and BIG

Final state	Model	$m^*$ [GeV]	$\langle \sigma v \rangle^*$ [cm <sup>3</sup> /s]	$LR$ (denom)	$LR$ (num)	$LR$	local signif. [ $\sigma$ ]
$b\bar{b}$	BIG	109.3	1.71e-26	48.37	51.65	3.28	1.8
$b\bar{b}$	SLIM	109.1	1.48e-26	48.77	51.70	2.93	1.7
$b\bar{b}$	QUAINT	106.7	4.28e-27	45.32	45.53	0.22	0.5
$q\bar{q}$	BIG	88.5	4.41e-27	50.31	51.65	1.35	1.2
$\mu^+\mu^-$	BIG	155.7	2.65e-23	49.76	51.65	1.90	1.4
$W^+W^-$	BIG	106.8	2.20e-26	49.24	51.65	2.41	1.6
$hh$	BIG	166.7	3.62e-26	49.28	51.65	2.38	1.5

dof = 54    56

Err. data / model	local signif. [ $\sigma$ ]	$m^*$ [GeV]	$\langle \sigma v \rangle^*$ [cm <sup>3</sup> /s]
cov/cov	1.81	109.3	1.71e-26
cov/none	2.39	10.5	5.07e-26
diag/cov	3.33	98.8	2.14e-26
diag/none	2.75	8.5	1.70e-25
stat/cov	5.19	89.7	1.48e-26
stat/none	4.49	8.0	2.98e-25

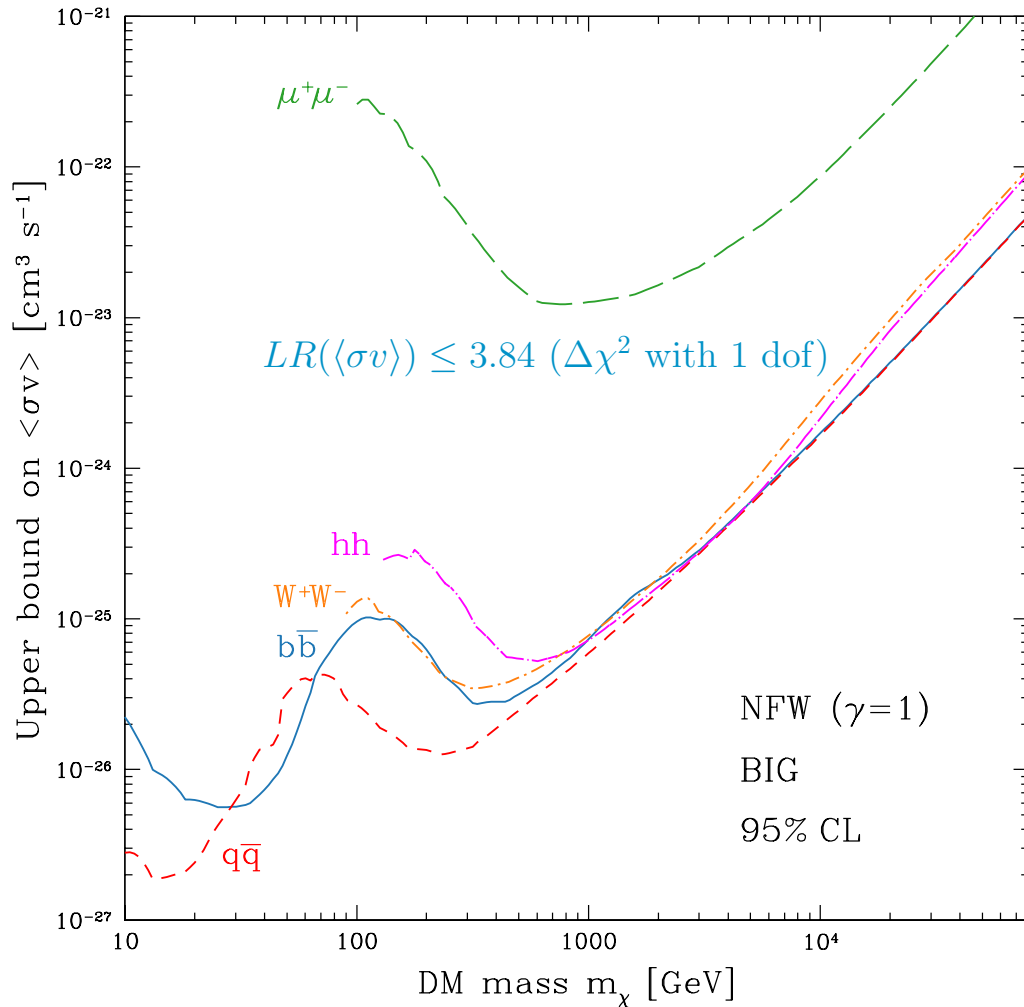
Significance of the fit w/wo  $\mathcal{C}^{\text{data}}$  and  $\mathcal{C}^{\text{model}}$

No statistical significance in favour of a DM signal in  $\bar{p}$  flux

# $\bar{p}$ – Bounds on DM and a word of caution

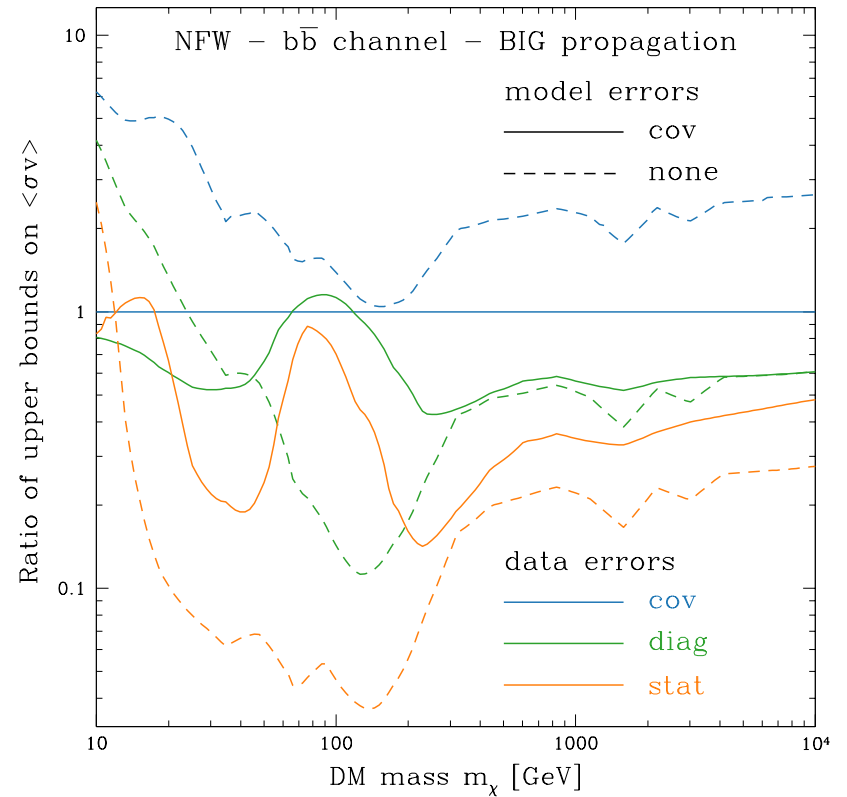
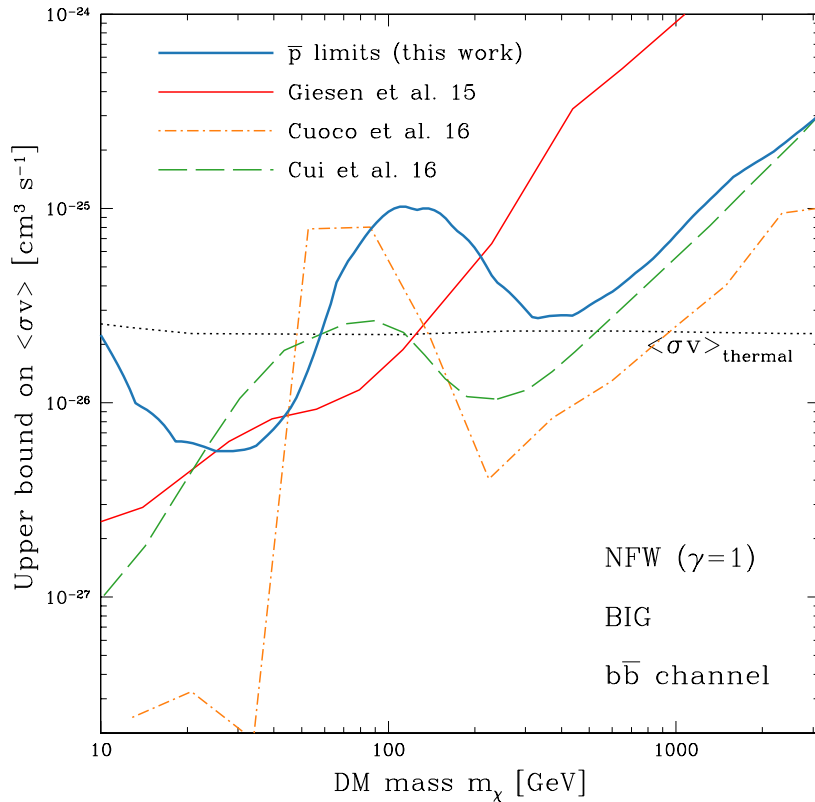
To set constraints on DM properties, we fix  $m_\chi$  and define the likelihood ratio

$$LR(\langle\sigma v\rangle) = -2\ln \mathcal{L}(L_{\min}, \langle\sigma v\rangle) + 2\ln \mathcal{L}(L', \langle\sigma v\rangle')$$



# $\bar{p}$ – Bounds on DM and a word of caution

Comparison with  $\bar{p}$  limits from other groups exhibits some differences.



$$\text{Covariance matrix } \mathcal{C} = \left\{ \mathcal{C}^{\text{data}} \text{ or } \sqrt{\sigma_{\text{stat}}^2 + \sigma_{\text{sys}}^2} \text{ or } \sigma_{\text{stat}} \right\} \oplus \left\{ \mathcal{C}^{\text{model}} \text{ or } 0 \right\}$$

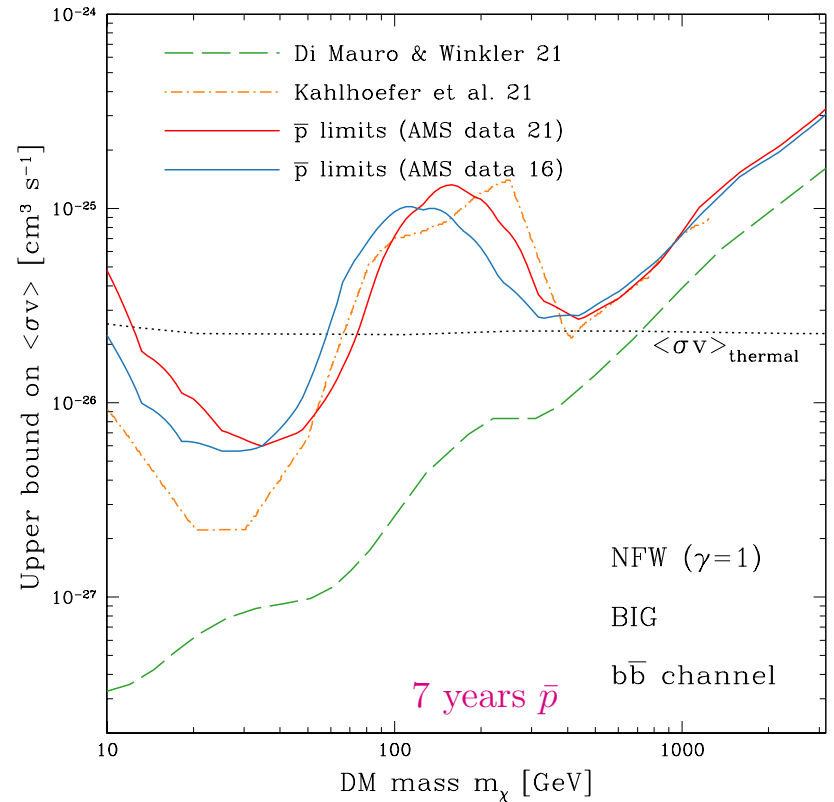
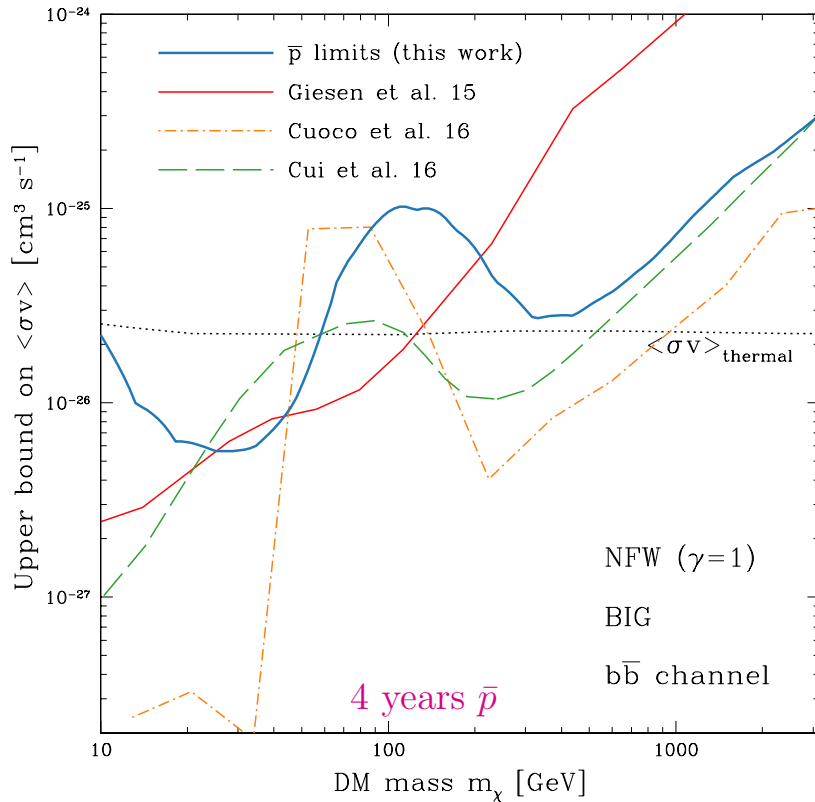
**A word of caution**

Errors should be now treated correctly with covariance matrices.



# $\bar{p}$ – Bounds on DM and a word of caution

Comparison with  $\bar{p}$  limits from other groups exhibits some differences.

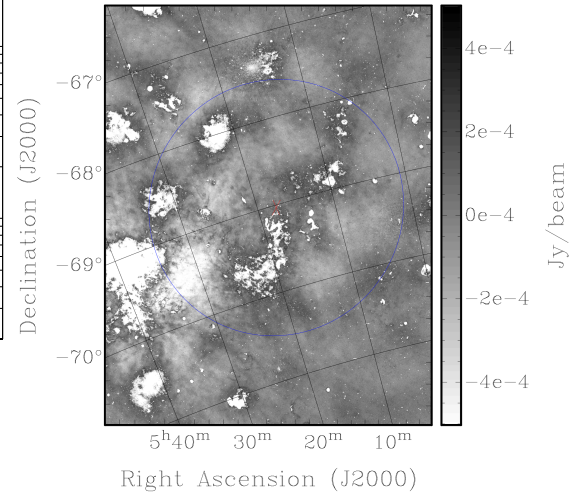
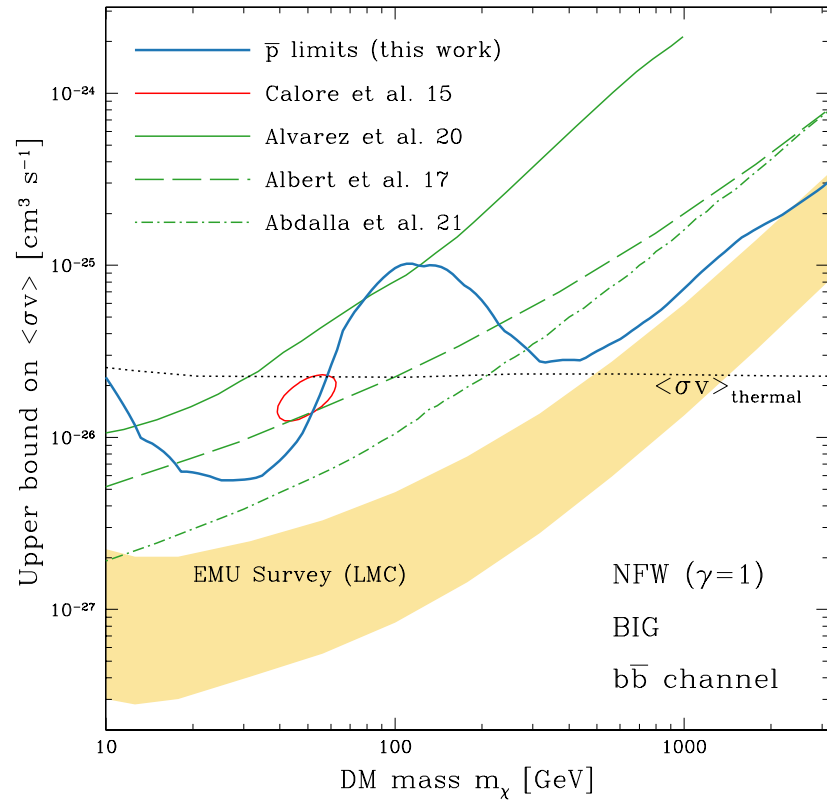
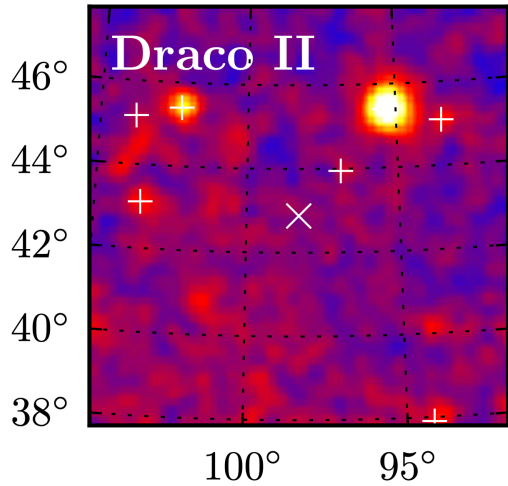


We qualitatively obtain the same bounds for the two  $\bar{p}$  AMS data sets published in [Aguilar+, PRL 117 \(2016\) 091103](#) & [Aguilar+, Phys. Rept. 894 \(2021\) 1](#).

Excellent agreement with the bounds derived by [Kahlhoefer+\[2107.12395\]](#) using an extensive  $\Phi_{\bar{p}}$  library with neural networks (machine learning).

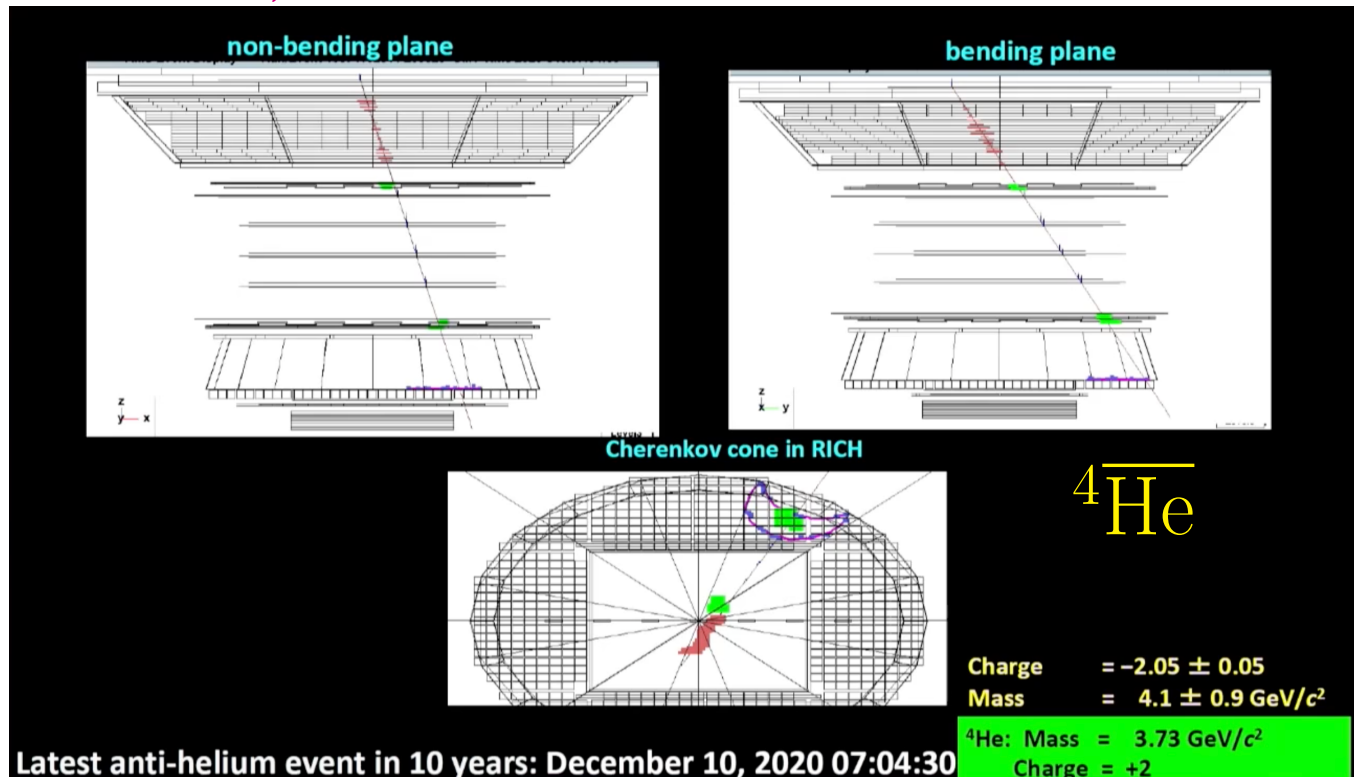
# $\bar{p}$ – Bounds on DM and a word of caution

The  $\bar{p}$  bound has a comparable strength to aggressive  $\gamma$ -ray bounds from dSph.



The  $\bar{p}$  flux probes deeply into the DM parameter space and sets strong bounds.

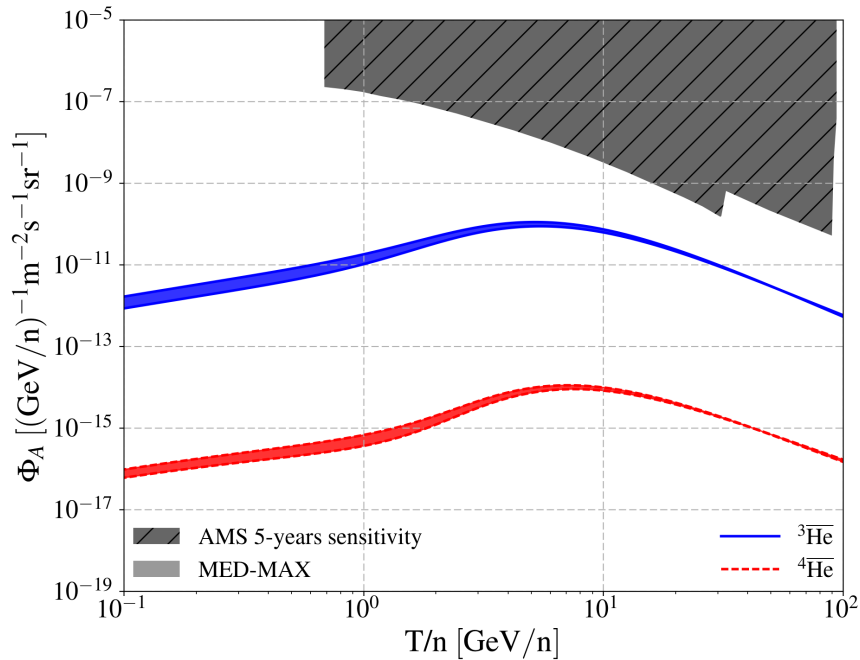
## 5) Anti-He nuclei – The new frontier



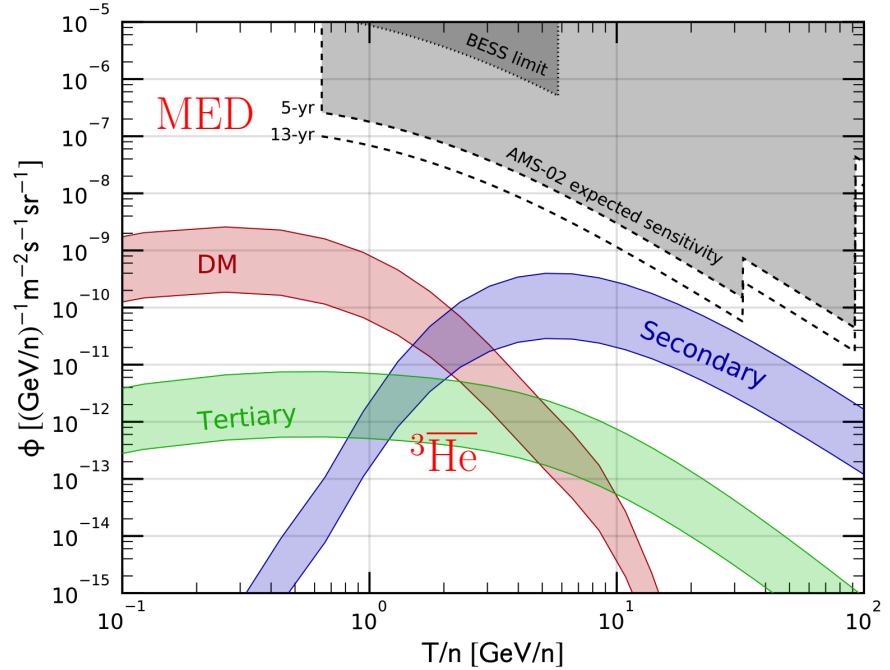
V. Choutko, Cosmic Heavy Anti-Matter, COSPAR E1.3-05-22, July 17th 2022

- AMS-02 has observed few events in the mass region from 0 to 10 GeV with charge  $Z = -2$  and rigidity  $\mathcal{R} < 50$  GV. The masses of all events are in the  ${}^3\overline{\text{He}}$  and  ${}^4\overline{\text{He}}$  mass region.
- The event rate is 1 anti-helium in  $\sim 100$  million helium.
- Massive MC background simulations are carried out to evaluate significance. So far 35 billion He events simulated vs 6.8 billion He event triggers for 10 years. AMS-02 did not find background to the anti-helium events. At this level, the MC simulations are difficult to validate.

# Secondary anti-helium fluxes



Poulin+[1808.08961]



Korsmeier+[1711.08465]

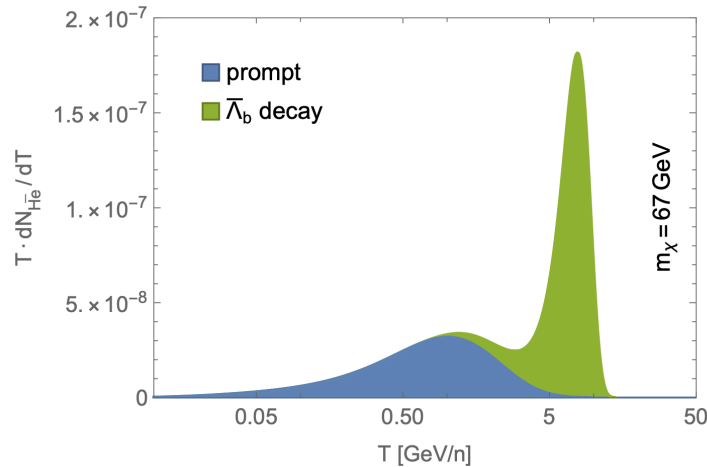
- Interactions of high-energy cosmic-ray protons and helium nuclei on the ISM yield a **secondary anti-He flux** well below AMS-02 sensitivity.
- The same conclusion holds for DM decays or annihilations although M. Winkler and T. Linden have proposed a nice counter-example based on  $\bar{\Lambda}_b$  production if pure  ${}^3\bar{\text{He}}$  events – [Winkler+\[2006.16251\]](#).
- The General Antiparticle Spectrometer (GAPS) is about to fly and measure the  $\bar{p}$  flux below 200 MeV). GAPS has a cute way to disentangle  $\bar{p}$  from  $\bar{d}$  – [See Aramaki's talk](#).

# A new scenario for $\overline{^3\text{He}}$ production from DM

- In general, DM species annihilations do not produce a detectable amount of antihelium nuclei  $\overline{^3\text{He}}$ .
- Since DM is at rest, the spectrum peaks at low energy  $\neq \mathcal{O}(10)$  GeV/n.
- Recently, a new proposal based on DM coupling to  $b$  quarks.

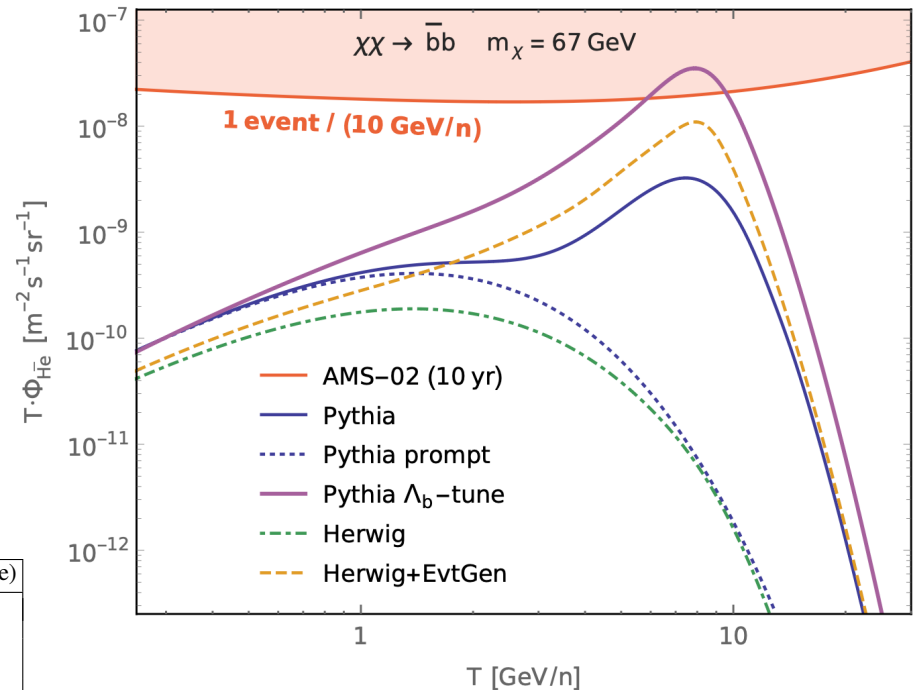
$$\chi + \chi \rightarrow b + \bar{b} \quad \bar{b} \rightarrow \bar{\Lambda}_b \text{ meson}$$

$$\bar{\Lambda}_b (5.6 \text{ GeV}) \rightarrow \overline{^3\text{He}} (4.7 \text{ GeV})$$



$$\bar{\Lambda}_b \rightarrow \bar{d} u \bar{u} (\overline{ud})_0$$

experiment	channel	measurement	Pythia (default)	Pythia ( $\Lambda_b$ -tune)
LEP [4, 5]	$f(b \rightarrow \Lambda_b)$	$0.101^{+0.039}_{-0.031}$	0.037	0.101
LEP [6]	$f(b \rightarrow \Lambda_b, \Xi_b, \Omega_b)$	$0.117 \pm 0.021$	0.047	0.127
Tevatron CDF [7]	$\frac{f(b \rightarrow \Lambda_b)}{f(b \rightarrow B)}$	$0.281^{+0.141}_{-0.103}$	0.046	0.135
LHCb [8]	$\frac{f(b \rightarrow \Lambda_b)}{f(b \rightarrow B)}$	$0.259 \pm 0.018$	0.048	0.134



Winkler+[2006.16251]

# Charged-particle

## What charged cosmic rays tell us on dark matter

### Takeaway

- The transport of charged particles inside the magnetic halo of the Galaxy is better understood, especially in the light of recent AMS-02 observations. The size of the magnetic halo  $L$  is measured to be  $4.5 \pm 1$  kpc.
- Anomalies in the fluxes of antimatter charged cosmic rays could be an indirect signature of annihilating DM particles. **But caution must prevail.** Positrons, for instance, are most probably accelerated in PWNe and are detected as  $\gamma$ -ray TeV haloes.
- Many groups have reported a  $\bar{p}$  anomaly hinting at DM. But taking properly the errors into account, i.e. including their correlations, makes the excess recede.
- AMS-02 has reported a few anti-helium events. If confirmed, this would be a major discovery, pointing to exotic physics. If DM annihilates into  $b\bar{b}$  quarks, the decay of  $\bar{\Lambda}_b$  into  ${}^3\text{He}$  could produce an excess over secondaries.





# Charged-particle

## What charged cosmic rays tell us on dark matter

Thanks for your attention

- The transport of charged particles inside the magnetic halo of the Galaxy is better understood, especially in the light of recent AMS-02 observations. The size of the magnetic halo  $L$  is measured to be  $4.5 \pm 1$  kpc.
- Anomalies in the fluxes of antimatter charged cosmic rays could be an indirect signature of annihilating DM particles. **But caution must prevail.** Positrons, for instance, are most probably accelerated in PWNe and are detected as  $\gamma$ -ray TeV haloes.
- Many groups have reported a  $\bar{p}$  anomaly hinting at DM. But taking properly the errors into account, i.e. including their correlations, makes the excess recede.
- AMS-02 has reported a few anti-helium events. If confirmed, this would be a major discovery, pointing to exotic physics. If DM annihilates into  $b\bar{b}$  quarks, the decay of  $\bar{\Lambda}_b$  into  ${}^3\text{He}$  could produce an excess over secondaries.

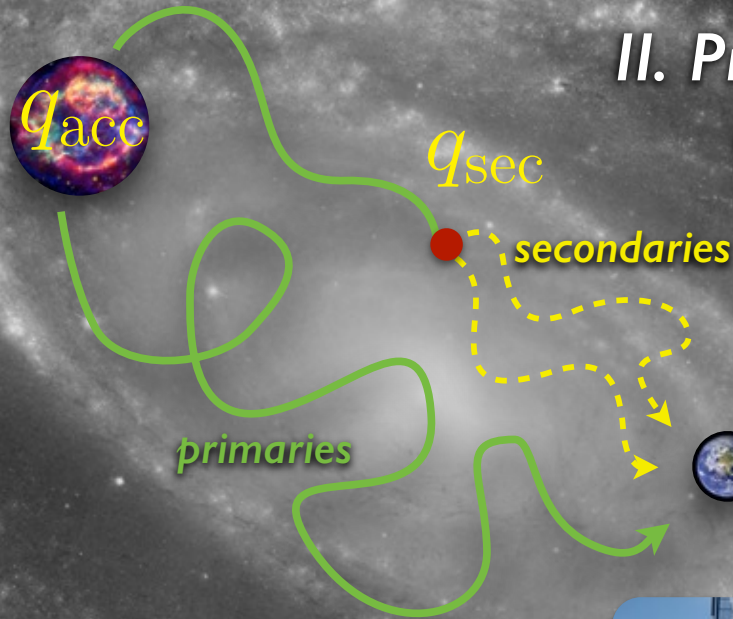


Back up slides

## 2) Measuring the height $L$ of the magnetic halo

### I. Sources & Acceleration

*diffusive shock acceleration*



### II. Propagation in the ISM

*diffusion, convection, re-acceleration*

### III. Solar System & Detection

*solar modulation, geomagnetic cut-off*

# Fitting CR nuclei – MCMC or MINUIT/MINOS

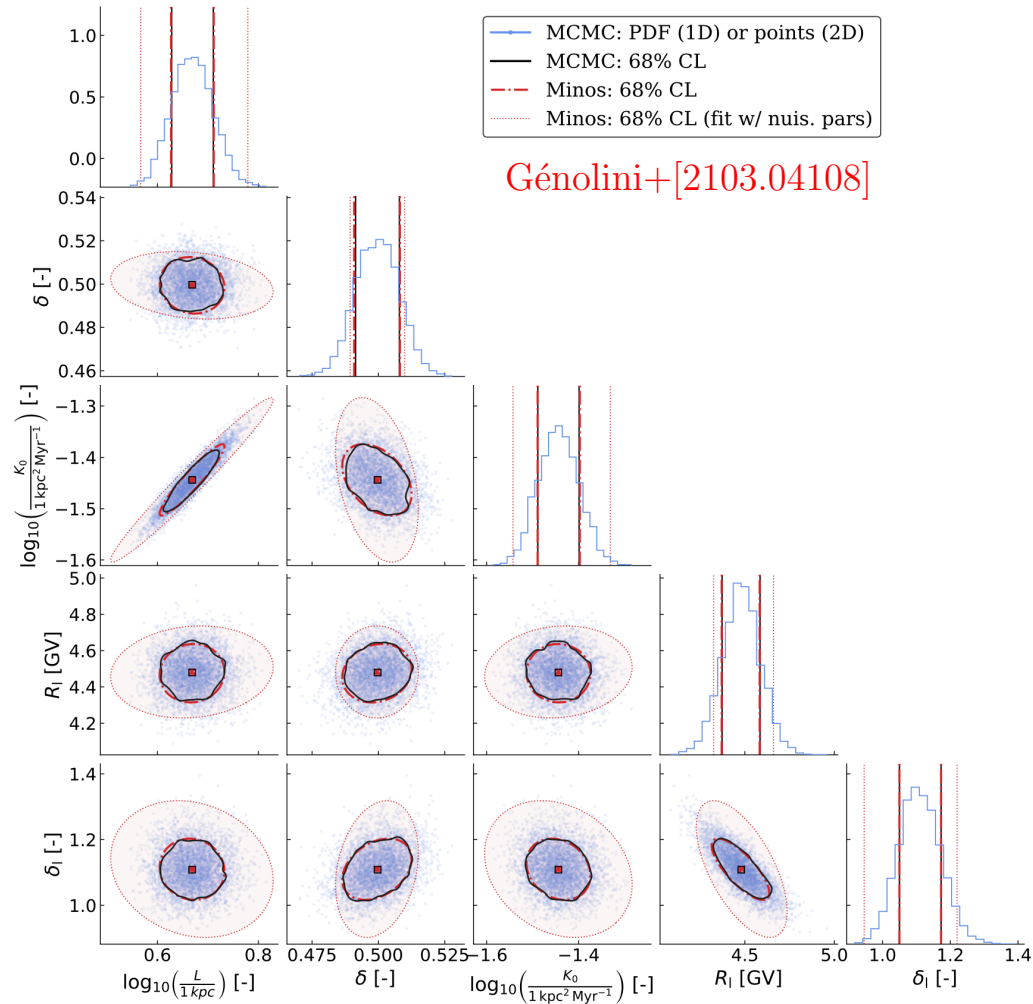
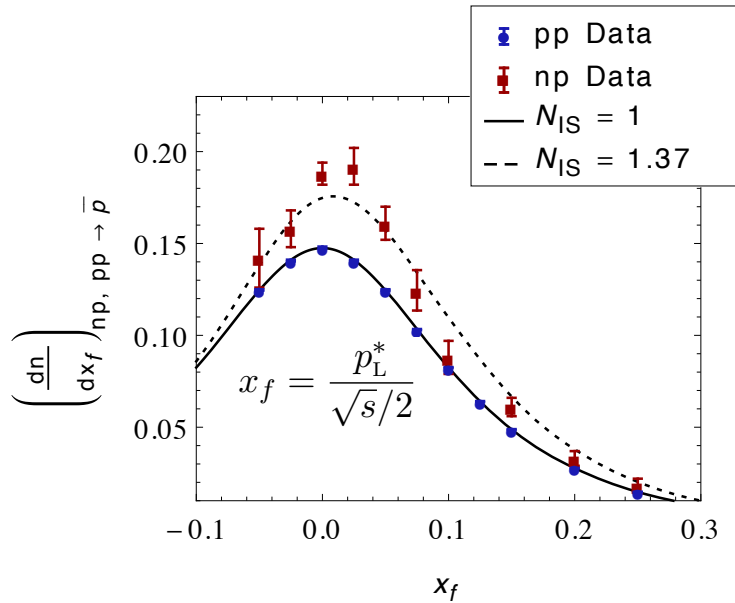


FIG. 7: Comparison of constraints on transport parameters obtained from an MCMC engine or via the HESSE-MINOS algorithms. In off-diagonal plots, the black squares and red crosses show the best-fit values from the former and latter results respectively, MCMC points are shown in blue (from which 68% confidence level contours are extracted in black), and red ellipses are based on symmetrized MINOS errors (dash-dotted or dotted lines for the fit accounting for nuisance parameters). In diagonal plots, the blue histograms corresponds to the 1D probability distribution function (MCMC), and the 68% CL contours are shown as vertical blue lines (MCMC) and red vertical lines (HESSE-MINOS). We recall that the 1D 68% CL on any given parameter is not expected to match the projected value obtained from the 2D 68% CL. See text for discussion.

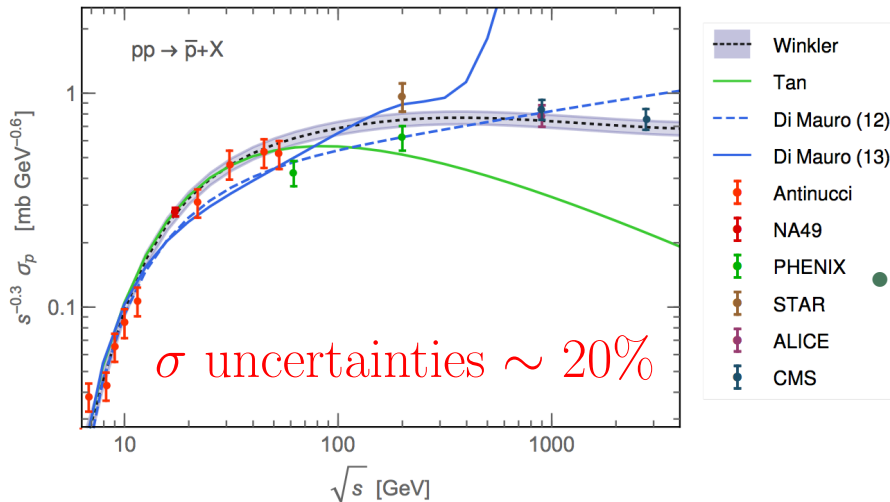
# $\bar{p}$ production cross section uncertainties



R. Kappl & M.W. Winkler, JCAP **1409** (2014) 051

M.W. Winkler, JCAP **1702** (2017) 048

A. Reinert & M.W. Winkler, JCAP **1801** (2018) 055



$$\frac{d\sigma_{pH \rightarrow \bar{p}}}{dE_{\bar{p}}}(E_p, E_{\bar{p}}) = p_{\bar{p}} \int d\Omega \left\{ \sigma_{\text{inv}} \equiv E_{\bar{p}} \frac{d^3\sigma}{d^3p_{\bar{p}}}(\sqrt{s}, x_R, p_{\bar{p}}^T) \right\}$$

- Anti-hyperons eventually decay in space

$$p + p \rightarrow \{\bar{\Lambda} \rightarrow \bar{p}\} + X$$

- Isospin asymmetry

$$p + p \rightarrow \{\bar{n} \rightarrow \bar{p}\} + X$$

$$\sigma_{pH \rightarrow \bar{n}} = N_{IS} \times \sigma_{pH \rightarrow \bar{p}}$$

- Interactions between nuclei heavier than  $p$

data from NA49 ( $p + C$ ) & LHCb ( $p + He$ )

- Fit to data with analytic parameterisations

- NA49 (2014) @  $\sqrt{s} = 13.7$  GeV

- NA61 (2017) @  $\sqrt{s} = 7.7, 8.8, 12.3$  &  $13.7$  GeV

M. di Mauro et al., Phys. Rev. **D90** (2014) 085017

M. Korsmeier et al., Phys. Rev. **D97** (2018) 103019

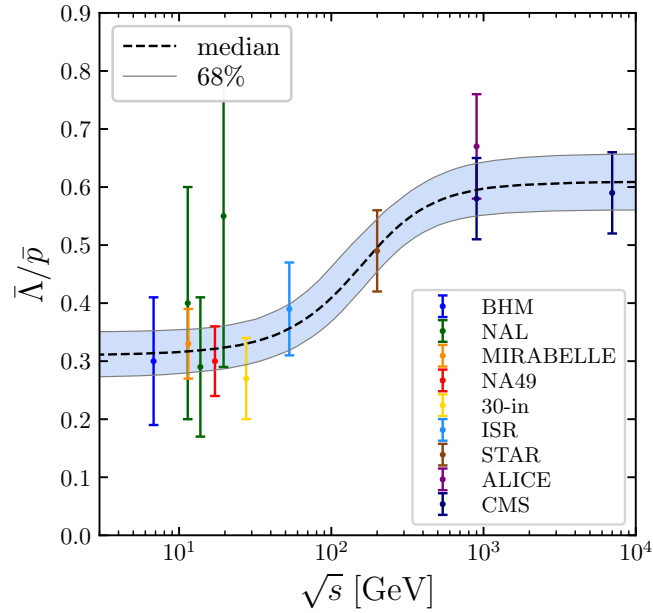
- Monte Carlo tools EPOS-LHC & QGSJET-II-04

- tuned on CR air showers with HE interactions

- poor description for  $E_{\bar{p}} \leq 50$  GeV

M. Kachelriess et al., Astrophys. J. **803** (2015) 54

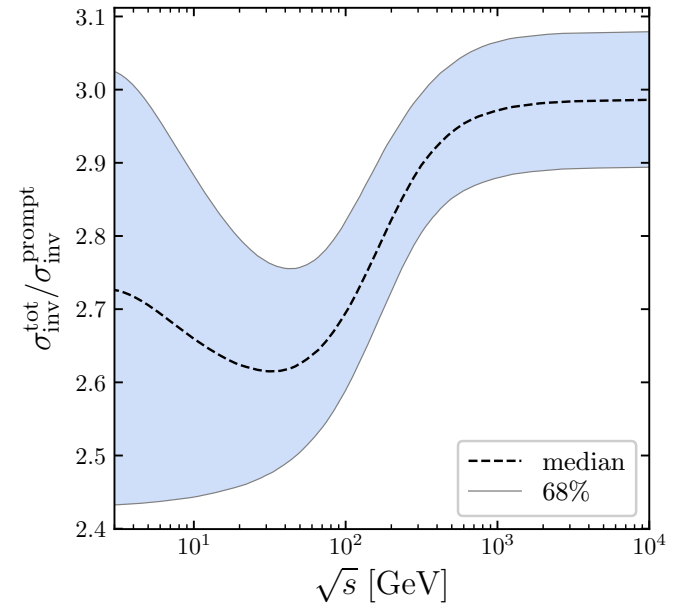
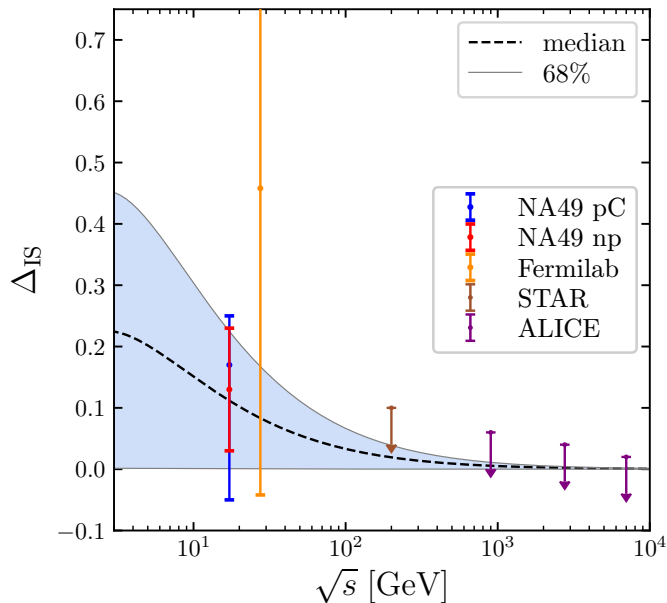
# $\bar{p}$ production cross section uncertainties



$$\frac{d\sigma_{pH \rightarrow \bar{p}}}{dE_{\bar{p}}}(E_p, E_{\bar{p}}) = p_{\bar{p}} \int d\Omega \left\{ \sigma_{\text{inv}} \equiv E_{\bar{p}} \frac{d^3\sigma}{d^3p_{\bar{p}}}(\sqrt{s}, x_R, p_{\bar{p}}^T) \right\}$$

$$\Delta_{\Lambda} = \frac{\bar{\Lambda}}{\bar{p}} \times \text{Br}(\bar{\Lambda} \rightarrow \bar{p} + \pi^+) + \frac{\bar{\Sigma}^-}{\bar{p}} \times \text{Br}(\bar{\Sigma}^- \rightarrow \bar{p} + \pi^0)$$

$$\sigma_{\text{inv}}^{\text{tot}} = \sigma_{\text{inv}}(2 + \Delta_{\text{IS}} + 2\Delta_{\Lambda})$$



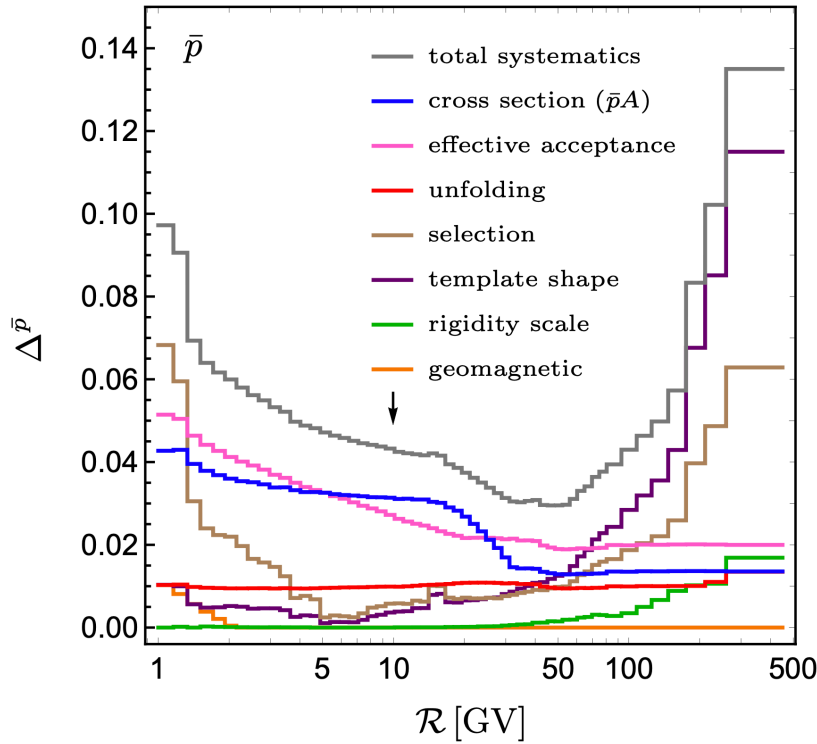
Boudaud+[1906.07119]



# $\bar{p}$ – Exploring the null hypothesis in search for DM

Results vary among authors. Errors on  $\bar{p}$  flux should be dealt with great care.

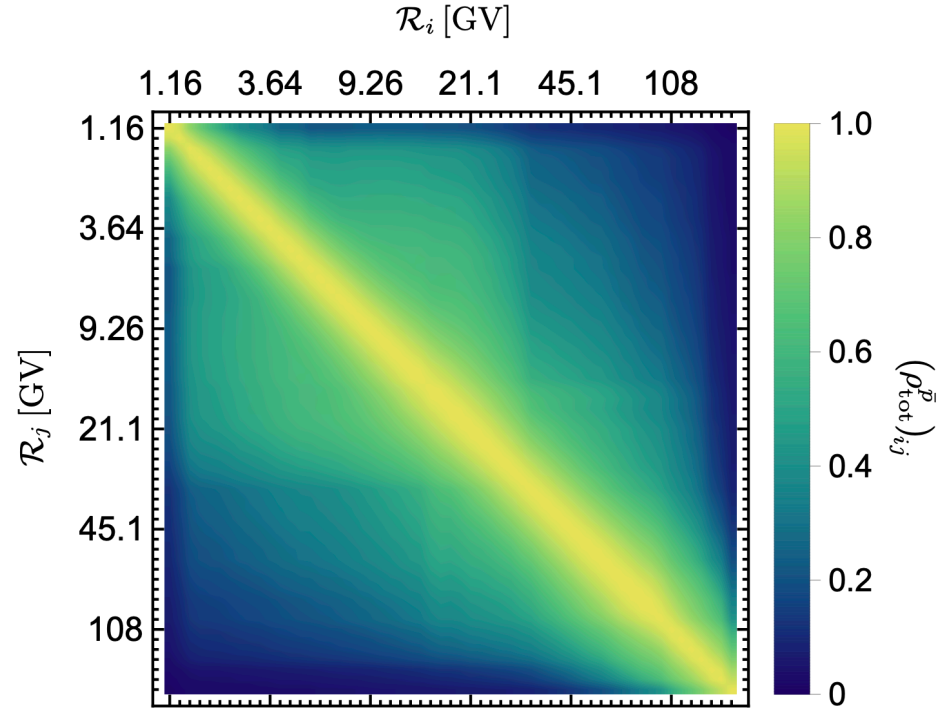
$$\chi_{\bar{p}}^2 \equiv x_i (\mathcal{C}^{-1})_{ij} x_j \quad \text{where} \quad x_i = \Phi_{\bar{p},i}^{\text{exp}} - \Phi_{\bar{p},i}^{\text{th}} \quad \text{while} \quad \mathcal{C} = \mathcal{C}^{\text{data}} + \mathcal{C}^{\text{model}}$$



$$l_{\text{eff. acc.}} = 0.15$$

$$l_{\text{scale}} = 4, \quad l_{\text{unf}} = 1, \quad l_{\text{geo}} = 1$$

$$l_{\text{selection}} = 0.5, \quad l_{\text{template}} = 0.5$$

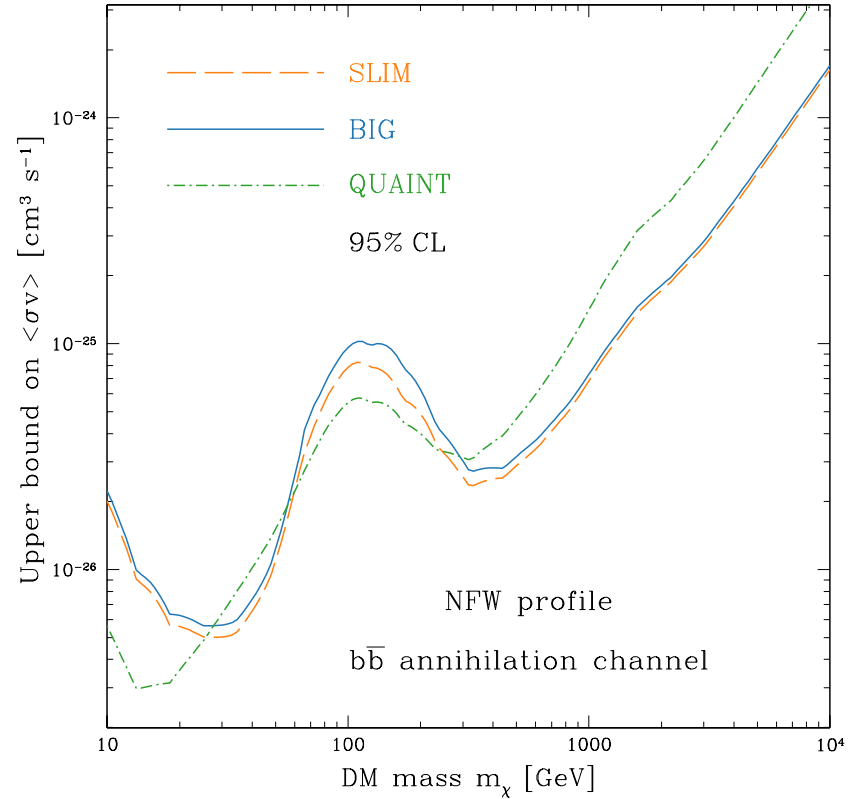
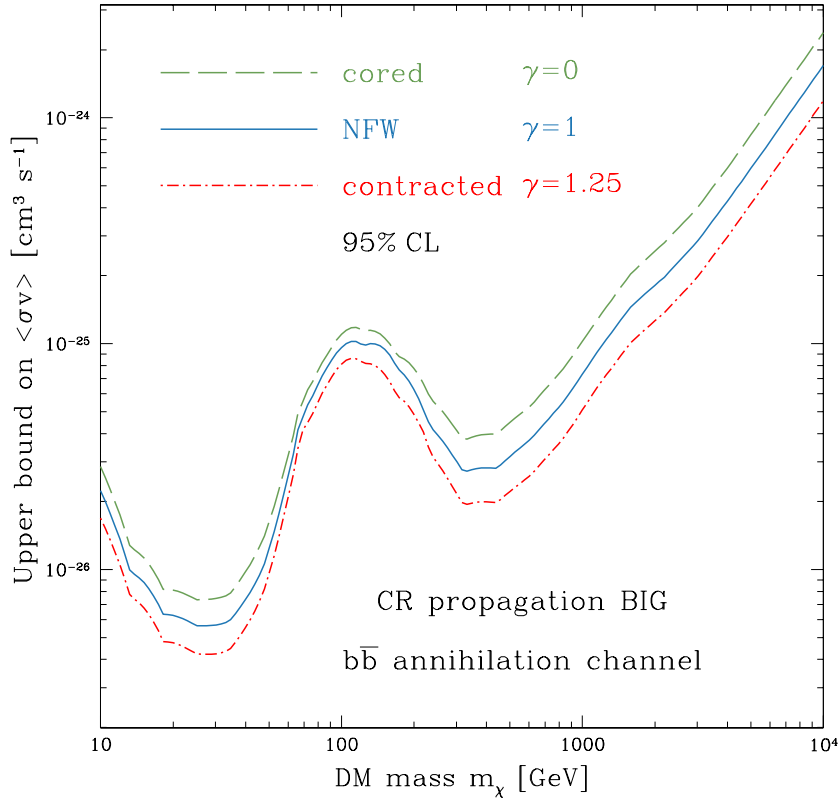


data correlation matrix

$$c_{ij}^{\alpha} \equiv \rho_{ij}^{\alpha} = \exp \left[ -\frac{1}{2} \left\{ \frac{\log_{10}(\mathcal{R}_i / \mathcal{R}_j)}{l_{\alpha}} \right\}^2 \right]$$

# $\bar{p}$ – Bounds on DM and a word of caution

To constraints mildly depend on DM profile and CR propagation.



$$\rho_{\text{DM}}(r) = \frac{\rho_s}{(r/r_s)^\gamma (1 + r/r_s)^{3-\gamma}}$$

Profile	$\gamma$	$r_s$ [kpc]	$\rho_s [M_\odot/\text{pc}^3]$
benchmark NFW	1.0	19.6	0.00854
cored	0.0	7.7	0.08931
contracted NFW	1.25	27.2	0.00361

	BIG	SLIM	QUANT
<b>Base &amp; Be/B (AMS-02)</b>			
$L$ [kpc]	$4.96^{+2.97}_{-1.76}$	$5.04^{+3.07}_{-1.79}$	$4.79^{+3.19}_{-1.77}$
$\chi^2 / n_{\text{dof}}$	233.7 / 193	233.1 / 195	235.3 / 194
$\chi^2_{\text{nui}} / n_{\text{nui}}$	17.4 / 20	17.4 / 20	15.8 / 20

# $\bar{p}$ – Changing the Fisk potential

